HHS Public Access

Author manuscript

Neuropharmacology. Author manuscript; available in PMC 2022 July 01.

Published in final edited form as:

Neuropharmacology. 2021 July 01; 192: 108603. doi:10.1016/j.neuropharm.2021.108603.

BK channel-forming slo1 proteins mediate the brain artery constriction evoked by the neurosteroid pregnenolone

Kelsey C. North, **Anna N. Bukiya**, **Alex M. Dopico**

Department of Pharmacology, Addiction Science and Toxicology, College of Medicine, The University of Tennessee Health Science Center, Memphis, TN, 38103

Abstract

Pregnenolone is a neurosteroid that modulates glial growth and differentiation, neuronal firing, and several brain functions, these effects being attributed to pregnenolone actions on the neurons and glial cells themselves. Despite the vital role of the cerebral circulation for brain function and the fact that pregnenolone is a vasoactive agent, pregnenolone action on brain arteries remain unknown. Here, we obtained *in vivo* concentration response curves to pregnenolone on middle cerebral arteries (MCA) diameter in anesthetized male and female C57BL/6J mice. In both male and female animals, pregnenolone (1 nM-100 μM) constricted MCA in a concentration-dependent manner, its maximal effect reaching ~22–35% decrease in diameter. Pregnenolone action was replicated in intact and de-endothelialized, *in vitro* pressurized MCA segments with pregnenolone evoking similar constriction in intact and de-endothelialized MCA. Neurosteroid action was abolished by 1 μM paxilline, a selective blocker of Ca^{2+} - and voltage-gated K^+ channels of large conductance (BK). Cell-attached, patch-clamp recordings on freshly isolated smooth muscle cells from mouse MCAs demonstrated that pregnenolone at concentrations that constricted MCAs *in vitro* and *in vivo* (10 μM), reduced BK activity (NPo), with an average decrease in NPo reaching 24.2%. The concentration-dependence of pregnenolone constriction of brain arteries and inhibition of BK activity in intact cells were paralleled by data obtained in cell-free, inside-out patches, with maximal inhibition reached at 10 μM pregnenolone. MCA smooth muscle BKs include channel-forming α (slo1 proteins) and regulatory β_1 subunits, encoded by *KCNMA1* and *KCNMB1,* respectively. However, pregnenolone-driven decrease in NPo was still evident in MCA myocytes from *KCNMB1*$^{-/-}$ mice. Following reconstitution of slo1 channels into artificial, binary phospholipid bilayers, 10 μM pregnenolone evoked slo1 NPo inhibition which was similar to that seen in native membranes. Lastly, pregnenolone failed to constrict MCA from *KCNMA1*$^{-/-}$ mice. In conclusion, pregnenolone constricts MCA independently of neuronal, glial, endothelial and circulating factors, as well as of cell integrity, organelles, complex membrane cytoarchitecture, and the continuous presence of cytosolic signals. Rather, this action involves direct inhibition of SM BK channels, which does not require β_1 subunits but is mediated through direct sensing of the neurosteroid by the channel-forming α subunit.

Correspondence: Alex Dopico, M.D., Ph.D., Dept. Pharmacology, Addiction Science and Toxicology, College of Medicine, The University of Tennessee Health Science, Center, 71 S. Manassas St, Room #231, Memphis TN 38103, Phone: 1(901) 448-3822, adopico@uthsc.edu.

Keywords

pregnenolone; neurosteroid; brain arteries; calcium-activated potassium channels; voltage-gated potassium channels; cerebral artery constriction

1.1 Introduction

Pregnenolone (PREG) is a local and circulating neurosteroid that regulates basic brain processes, such as neuronal firing and growth and differentiation of glial cells (Mayo et al., 2003, 2005; Masuyama et al., 2016). Moreover, many studies indicate that prevalent brain conditions such as depression and anxiety, alcohol use disorders, stress responses and even Alzheimer progression are related to and could be modified through optimization of PREG (or its analog allopregnanolone) levels (Akan et al., 2008; Akwa, 2020; Finn et al., 2004; Lejri et al., 2019; Mayo et al., 2003, 2005; Porcu and Morrow, 2014). PREG effects on the brain have been solely attributed to PREG actions on receptors and ion channels located in the neuron and glia cell themselves (Akan et al., 2008; Mayo et al., 2003, 2005; Masuyama et al., 2016). Despite the vital role of an optimal artery diameter for brain function (Faraci et al., 1998; González et al., 2012; Tano et al., 2014), and the fact that PREG is a vasoactive agent in the peripheral circulation (Figueroa-Valverde et al., 2009, 2014), studies of PREG on brain artery function are unavailable.

PREG modification of peripheral artery diameter has been attributed to PREG recognition by cytosolic and membrane steroid receptors and their downstream signaling (Chen et al., 1999; Kublickiene et al., 2008; McCurley et al., 2013). However, the modification of physiology, including vascular physiology, through lipid (including steroids)-ion channel protein direct interactions is a growing area of research (Dopico and Bukiya, 2014; Antollini and Barrantes, 2016; Taylor and Sanders, 2016).

In mammals, the Ca^{2+}- and voltage-gated K^+ channels of large conductance (BK) that prevail in cerebral artery smooth muscle (SM) include channel-forming α(slo1 proteins) and regulatory β_1 subunits (Dopico et al., 2018). The latter show localized expression in SM (Orio et al., 2002; Li and Yan, 2016) suiting BK function to SM-specific physiology. Thus, β_1 increases the apparent Ca^{2+}-sensitivity of BK, allowing this channel to oppose depolarization-mediated Ca^{2+} influx, limit SM contraction, and favor artery dilation (Brayden and Nelson, 1992; Orio et al., 2002). The abundant expression of β_1 in SM makes of this auxiliary subunit an important target of endogenous vasoactive lipids, including steroids (Dopico and Bukiya, 2014; Bukiya and Dopico, 2019). Thus, this regulatory subunit is necessary for the activation of BK channels by estradiol (Granados et al., 2019), and for channel activation and eventual cerebrovascular dilation by cholanes and derivatives (Bukiya et al., 2011, 2013). In contrast, slo1 subunits suffice for cholesterol, a precursor of PREG, to inhibit BK activity (Singh et al., 2012; Bukiya and Dopico, 2019).

Here, we tested the hypothesis that direct targeting of SM BK channel subunit(s) by PREG at physiological and pharmacological levels modified the diameter of middle cerebral arteries (MCAs). We focused on MCA because they perfuse the largest area within the brain, when compared to other cerebral arteries stemming from the circle of Willis and are the

more prone to neurovascular pathology (Cipolla and Curry, 2002; Navarro-Orozco and Sánchez-Manso, 2020).

2.1 Methods and Materials

2.2 Ethical Aspects of Research.

The care of animals and experimental protocols were reviewed and approved by the IACUC of the UTHSC, which is an institution accredited by the Association for Assessment and Accreditation of Laboratory Animal Care international.

2.3 Cerebral artery diameter measurement through cranial window *in vivo*.

8- to 12-week-old male and female C57BL/6 mice were anesthetized with a mixture of xylazine/ketamine (12/100mg per kg) and kept anesthetized for the duration of the experiment with subsequent ketamine doses (50mg/kg of weight) as needed. A catheter was inserted into the carotid artery so that the infusion went straight to the brain rather than towards the thoracic cavity. An area of the skull was cleared of tissue and thinned to expose the branching arteries originating from the MCA on the side the catheter was inserted, above the zygomatic arch, between the ear and eye of the skull (Busija and Leffler, 1991). The exposed arteries branching out from the MCA were monitored using a Leica MC170 HD microscope with a mounted camera (Leica M125 C) connected to a computer monitor. Drugs were diluted to their final concentration in sodium saline (0.9% NaCl) and administered via catheter at 0.1 mL/25 g of weight. Cranial window images before and after drug administration were acquired every 60 seconds for subsequent analysis.

2.4 Cerebral artery diameter measurement *in vitro.*

8- to 12-week-old C57BL/6J and *KCNMA1*$^{-/-}$ on C57BL/6 background mice of both sexes were deeply anesthetized with isoflurane via inhalation in a tightly sealed jar. Resistance-size MCAs (~100 μm in external diameter) were dissected out of the mouse brains after animal euthanasia with sharp scissors. For de-endothelialized records, the endothelium was removed by passing an air bubble into the vessel lumen for 90 seconds (Liu et al., 2004). This method has been consistently used by our group and validated using endothelium-dependent versus endothelium-independent vasodilators (Bukiya et al., 2007; Bukiya et al., 2011b). Arteries were cannulated as previously described by our group (Bukiya et al., 2011b; 2013). MCAs were cut into 5 to 10 mm-long segments under a microscope (Nikon SMZ645). The segment was cannulated at each end, and the artery exterior was continuously perfused with physiologic sodium saline (PSS) of the following composition (mM): 119 NaCl, 4.7 KCl, 1.2 KH2PO4, 1.6 $CaCl_2$, 1.2 MgSO4, 0.023 EDTA, 11 glucose, 24 $NaHCO_3$, pH=7.4. PSS was continuously bubbled with an $O_2/CO_2/N_2$ (21/5/74%) gas mixture and maintained at 35–37°C. The artery external wall diameter was measured using the automatic edge-detection function of lonWizard software (lonOptix) via Sanyo VCB-3512T camera (Sanyo Electric Co.). Arteries were first incubated at an intravascular pressure of 10 mm Hg for 10 min. Then intravascular pressure was increased to 60 mmHg and held steady throughout the experiment to induce myogenic tone development and maintenance (Liu et al., 2004; Bukiya et al., 2014). Each artery segment was exposed to PREG only once to avoid development of desensitization during repeated applications of PREG-containing

solution. When required by experimental design, arterial contractility was probed with a high KCl solution of the following composition (mM): 63.7 NaCl, 60 KCl, 1.2 KH_2PO_4, 1.2 $MgSO_4$, 0.023 EDTA, 11 glucose, 24 $NaHCO_3$, 1.6 $CaCl_2$, pH=7.4. Like PSS, the high-KCl solution was continuously bubbled with $O_2/CO_2/N_2$ (21/5/74%) gas mixture and maintained at 35–37°C.

2.5 Electrophysiology data acquisition and analysis.

Myocytes were isolated from 8- to 12- week-old C57BL/6 or *KCNMB1*$^{-/-}$ on C57BL/6 background male mouse MCAs as described (Bukiya et al., 2011a). Ionic currents were recorded in the cell-attached (C/A) configuration and from excised, inside-out (I/O) patches. C/A recordings were obtained at −30 mV, that is a physiologically relevant membrane voltage (Dopico et al., 2018). I/O recordings were obtained at +30 mV to evoke robust (sub-maximal) currents, so the inhibitory effect of PREG could be observed better. Bath and electrode solutions contained (mM): 130 KCl, 5 EGTA, 1.6 HEDTA, 2.28 $MgCl_2$ ([Mg^{2+}] free=1 mM), 15 HEPES; pH 7.40. In all experiments, free [Ca^{2+}] in solution was adjusted to the desired value by adding 1 mM $CaCl_2$ stock. An agar bridge with Cl^- as main anion was used as ground electrode. Solutions were applied onto the extra-patch myocyte surface of C/A or the cytosolic side of I/O patches using an automated, pressurized Octaflow system (ALA Scientific Instruments Inc.) through a micropipette tip with an internal diameter of 100 μm. Experiments were carried out at room temperature (20–22 °C). Ionic currents at single channel resolution were recorded using an EPC8 amplifier (HEKA) at 1 kHz. Data were digitized at 5 kHz using a Digidata 1320A A/D converter and pCLAMP 8.0 (Molecular Devices).

2.6 Preparation of slo1 protein.

BK channel-forming slo1 cDNA *(cbv1;* AY330293) was cloned from rat cerebral artery myocytes (Jaggar et al., 2005). Cbv1 cDNA was inserted into the pcDNA3.1 plasmid vector as described (Singh et al., 2012). CHO (Chinese hamster ovary) cells were transiently transfected with cbv1-carrying pcDNA3.1 plasmid using Lipofectamine 2000 (Invitrogen), grown to confluence, pelleted, and re-suspended on ice in 10 ml of buffer solution of the following composition (mM): 30 KCl, 2 $MgCl_2$, 10 HEPES, 5 EGTA; pH 7.2. A membrane preparation was obtained using a sucrose gradient as previously described (Crowley et al., 2003). Aliquots were stored at −80 °C. Slo1 current were recorded following protein reconstitution into planar lipid bilayers consisting of 1-palmitoyl-2-oleoyl-*sn*-glycero-3-phosphoethanolamine (POPE) and 1-palmitoyl-2-oleoyl-*sn*-glycero-3-phospho-l-serine (POPS) 3:1 (w/w) mixture. Lipid mixtures were dried under N_2 gas and re-suspended at 25 mg/ml of n-decane. Vertical bilayers (80–120 pF) were formed by painting the lipid mix across a 200 μm diameter hole in a deldrin cup (Warner Instruments). Membrane preparation of slo1 protein was added to the *cis* chamber, and fusion between the membrane preparation and the bilayer was promoted by osmosis, with the *cis* chamber recording solution being hyperosmotic to the *trans* chamber solution. Solution for the *cis* chamber contained (mM): 300 KCl, 10 HEPES; pH 7.2. Solution for the *trans* chamber contained (mM): 30 KCl, 10 HEPES, pH 7.2. In all experiments, free [Ca^{2+}] in the solutions bathing both chambers was the same and adjusted to the desired nominal value as described above (Section 2.5). The *trans* chamber was held at ground (equivalent to the extracellular space) while the *cis*

chamber (equivalent to the intracellular space) was held at potentials relative to ground. Only channels with their intracellular Ca^{2+}-sensors oriented toward the *cis* chamber were considered for experimentation. Ion currents were obtained during 10-minute gap-free recording at +30 mV using a Warner BC-525D amplifier, low pass-filtered at 1 kHz using the 4-pole Bessel filter built into the amplifier and sampled at 5 kHz with Digidata 1322A/pCLAMP 8 (Molecular Devices). For proper comparisons with previous data obtained by us (Crowley et al., 2003; Bukiya et al., 2008; Bukiya et al., 2011a) and others (Chang et al., 1995; Yuan et al., 2007), studies were conducted at room temperature (20–22 °C). PREG stock or DMSO control was added to both *cis* and *trans* chambers to reach a final concentration of 10 μM in each chamber.

2.7 Chemicals.

PREG was purchased from Abcam. POPE, and POPS were purchased from Avanti Polar Lipids. All other chemicals were purchased from Sigma Aldrich. PREG and steroid blockers were dissolved in dimethyl sulfoxide (DMSO) and diluted into PSS solution immediately before application to the artery, myocyte membrane or bilayer. Each pressurized artery, myocyte membrane, or patch was exposed to PREG only once to avoid possible desensitization.

2.8 Data Analysis.

Changes in artery diameter obtained from cranial window experiments were determined using ImageJ software (ImageJ Downloaded from 9 1.52a, https://imagej.nih.gov/ij/download.html). *In vitro* MCA diameter data were analyzed using lonWizard 4.4 software (lonOptix) by continuous real time recording of the exterior diameter of cannulated artery segments. Each data point was collected on separate artery segments to avoid desensitization and false repetitions. Drug-induced effects in arterial diameter were determined at the maximal, steady drug concentration reached in the chamber before the perfusion was switched to another drug or a washout. The value for basal artery diameter (i.e., diameter before drug application) in both *in vivo* and *in vitro* experiments was obtained by averaging diameter values from the same arterial segment during 3 minutes of recording immediately before drug application. The concentration response curve data obtained from *in vivo* and *in vitro* experiments were fitted to a Boltzmann function of the type:

$$y = \frac{A_1 - A_2}{1 + e^{(x - x_0)/dx}} + A_2$$

using Origin 2020 software (OriginLab). Validity of the Bolzmann fit results is given by the corresponding reduced Chi-square and R-square values. Where the reduced Chi-square statistic is used to represent the goodness of fit testing (Wendt, 1991) and the R-square results evaluate the scatter of the data points around the fitted regression line (Freedman, 2009).

Patch-clamp and bilayer data were analyzed using Clampfit 10.7 software (Molecular Devices). NPo was used as an index of channel steady-state activity, where N=number of channels in the patch (defined as a maximal number of opening levels) and Po=single

channel open probability. Drug-induced NPo changes were determined by comparing baseline NPo (i.e., NPo with the patch/cell perfused with bath solution) to the NPo from the same patch/cell exposed to agent (DMSO/PREG/blockers) dissolved in bath solution.

Statistical analysis was performed using InStat 3.05 (GraphPad). When the number of observations in the groups under comparison exceeded 6, and the Gaussian distribution of the data was confirmed by the Kolmogorov-Smirnov test, analysis was performed using an unpaired Student's *t*-test. In all other cases, statistical analysis was conducted using the Mann-Whitney nonparametric test. For comparison of multiple experimental groups, the Kruskal-Wallis test with Dunn's post-test were used. In all cases, testing assumed two-tail P values with significance set at $P<0.05$.

3.1 Results

3.2 PREG is a cerebral artery constrictor *in vivo.*

In order to evaluate PREG action on male and female MCA at the organismal level, we used a cranial window. This technique allowed us to continuously monitor the external diameter of resistance-size pial arteries that arise from the MCA, as previously done to evaluate the alcohol pharmacology of these vessels (Busija and Leffler, 1991; North et al., 2020). For each experiment, baseline images of MCAs were captured prior to any drug application and used for reference of the fold-changes in MCA diameter throughout each experiment. All drugs were infused toward the cerebral circulation using an intra-carotid artery catheter as detailed in Material and Methods. PREG was tested at 0.001–100 μM, that is, a physiologically and pharmacologically relevant range of concentrations (Asscheman et al., 2014; Basar et al., 2005; Cutler and Laue, 1990; Akwa, 2020).

PREG-induced MCA constriction was concentration-dependent with EC_{50}=0.1 μM and maximal constriction (E_{max}) reached at 10 μM for male mice (Fig. 1A–C, reduced Chi-square=1.098, R-square=0.978). A similar concentration-dependent response to PREG was identified in female mice, with an EC_{50}=5 μM and E_{max}=100 μM (Fig. 1D–F, reduced Chi-square=0.01, R-square=0.999). An identical pattern was replicated in three to four animals for each PREG concentration, in male and female experimental groups. In all experiments, vehicle (DMSO) and saline controls failed to change MCA diameter (Fig. 1B, E). Averaged data shown in Fig. 1B–C, E–F reveal that PREG infusion-induced MCA constriction is evident immediately upon bolus injection of the drug; PREG evokes MCA diameter by 20–30% in male and by 18–24% in female mice. In both sexes, PREG-induced constriction reached statistical significance ($P<0.05$) by minute 7 when compared to either time-matched saline or DMSO infusion. Of note, there is no statistically significant difference in the maximal constriction by PREG in male versus female mice either. PREG-induced constriction remained sustained throughout 7 minutes of recording after injection, and statistically different ($P<0.05$) after minute 4 of recording time, when compared to time and volume matched injections of PREG's vehicle and saline. Thus, PREG is an effective constrictor of brain arteries *in vivo,* this action being similar in male and female animals.

3.3 PREG constricts cerebral arteries independent of circulating factors and functional endothelium.

In order to determine whether the vasoactive effects of PREG require circulating, paracrine, neuronal or glial factors or, rather, persist at the isolated organ level, MCA segments were *in vitro* pressurized and exposed to various concentrations of PREG (0.001–100 μM in males Fig. 2A–C; 1–100 μM in females Fig. 2D–F). Viability of isolated MCA segments was determined by evaluating their contraction in response to 60 mM KCl-induced depolarization (which serves as reader of close-to-maximal, depolarization-driven constriction; Liu et al., 2004). PREG evoked a decrease in MCA diameter that was fully reversible at all concentrations upon washout with PSS (Fig. 2A, D). PREG action was concentration-dependent with EC_{50}=3 μM and E_{max}=100 μM, at which diameter decreased by 8.90±1.9% of baseline values for intact male arteries (Figs. 2B; reduced Chi-square=0.09, R-square=0.99). In female mice, PREG EC_{50}=5.6 μM with an E_{max}=10 μM, with an average decreased artery diameter of 6.8± 0.98% of the baseline (Fig. 2E; reduced Chi-square=0.01, R-square=0.66).

The possible contribution of endothelial integrity/endothelial factors to PREG-induced MCA constriction was determined by obtaining a concentration-response curve to this neurosteroid in MCA segments in which the endothelium was removed prior to vessel pressurization and drug exposure. MCA segment viability was determined as described above for endothelium-intact vessels. PREG was tested at 0.001–100 μM in male and at 1–100 μM PREG in female mice. PREG constricted de-endothelialized MCAs from male mice in a concentration-dependent manner, with EC_{50}=1 μM and EC_{max}=10 μM, at which diameter decreased 7.6±0.83% of the pre-drug baseline (Fig. 2A, C; reduced Chi-square=0.28, R-square=0.99). In female de-endothelialized MCAs PREG constricted arteries with an EC_{50}=3 μM and E_{max}=10 μM, with a reduction in artery diameter of 2.5±0.29% from the pre-drug baseline (Fig. 2D;2F; reduced Chi-square=0.0, R-square=0.84). In MCAs from both male and female mice, the effect of PREG, at all concentrations, was fully washable upon PREG removal from artery perfusion chamber. Maximal constriction by PREG in intact and de-endothelialized MCAs was similar in male and female mice, strongly suggesting that the efficacy of PREG-induced constriction is sex-independent. Our data clearly underscore that the endothelium is not necessary for PREG to evoke MCA constriction.

3.4 PREG-induced constriction of cerebral arteries is driven by BK channel inhibition in cerebrovascular smooth muscle.

Since PREG is effective in constricting intact and de-endothelialized MCAs of male and female mice, the primary targets of PREG-induced cerebral constriction should be of extra-endothelial location. In de-endothelialized arteries, SM accounts for over 50% of total cellular content (Lee, 1995) and thus, may harbor the primary targets of PREG-induced vasoconstriction. In the periphery, ion channels and G protein-coupled steroid receptors are both known targets of PREG vascular actions (Figueroa-Valverde et al., 2009, 2014; Mayo et al., 2003, 2005; Rizvi et al., 2013; Akwa, 2020). However, PREG-activated steroid receptors usually result in vasodilation (Figueroa-Valverde et al., 2009;2014). In contrast, SM BK channel inhibition renders both peripheral and cerebrovascular constriction (Dopico et al., 2018). Therefore, we tested whether the BK channel was the main contributor to PREG-

induced constriction of de-endothelialized MCAs in male and female mice. Thus, we evaluated PREG action at its highest efficacious concentration (10 μM) in the presence of paxilline at a concentration that selectively blocks BK channels (1 μM; Strøbæk et al., 1996; Zhou and Lingle, 2014) and/or a mixture of drugs at concentrations that effectively block several known PREG targets: 20 μM ketoconazole to block pregnane X receptor (PXR), 33 μM MK-886 to block peroxisome proliferator-activated receptors (PPAR), and 20 μM mefenamic acid (MFA) to block the transient receptor potential cation channel subfamily M member 3 (TRPM3) (Amberg and Santana, 2003; Mayo et al., 2003, 2005; Rizvi et al., 2013; Zhou and Lingle, 2014). In de-endothelialized MCA segments, paxilline significantly reversed the arterial constriction by 10 μM PREG from 7.59±0.615 and 2.53±0.29% to dilation, reaching 0.81±0.38 and to 3.8±0.73 %, in males and females respectively (Fig. 3; P= 0.00114 (male), P= 0.00004 (female), Mann Whitney U-test). Moreover, the steroid blockers cocktail in presence of paxilline and 10 μM PREG reduced the dilation seen by paxilline to a nominal 1.4±0.5% and 1.01±1.1 %, for male and female respectively (Fig. 3). This also suggests that the minor dilatory effect seen with paxilline and PREG combined is caused by residual dilatory actions mediated by known steroid receptors.

To investigate PREG action on cerebrovascular BK channels themselves, we evaluated a possible PREG-induced BK current inhibition in C/A patches of intact SM cells freshly isolated from male MCA, these recordings obtained at physiological voltage (−30 mV; Pérez et al., 2001; Kuntamallappanavar et al., 2014). Since the concentration dependency and BK participation in PREG action remained consistently the same between male and female mice (see above), all patch-clamp electrophysiology was conducted on male mice to decrease the use and number of animals. To determine confirm the BK identity, each recording was followed by perfusion of 1 μM paxilline (Zhou and Lingle, 2014). Any record not significantly inhibited by perfusion of paxilline was excluded from analysis. Indeed, PREG significantly reduced BK activity immediately following neurosteroid application, an action that persisted throughout PREG perfusion when compared to time-matched perfusion with DMSO-containing solution (Fig. 4, P=0.02382, 0.00148, 0.00214, 0.0121, 0.0121, and 0.0121 for 1, 2, 3, 4, 5, and 6 minutes of perfusion, respectively; Mann Whitney U-test). Moreover, DMSO time- and concentration-matched control failed to inhibit BK channels, but rather caused a mild activation (Fig. 4A, 4C). Thus, our data in C/A patch configuration prove that PREG inhibits native BK channels in MCA myocytes.

Lastly, to determine whether PREG inhibition of BK channels persisted independently of cell signaling and internal organelles, we recorded BK channel openings in excised membrane patches with the I/O configuration of patch-clamp on freshly isolated mouse cerebral artery myocytes. I/O records were conducted at +30 mV to evoke high channel activity in order to assess the full degree of inhibition by a range PREG concentrations (0.01–100 μM) (Fig. 5). Indeed, PREG inhibited channel activity in a concentration-dependent manner (Fig. 5). Maximum inhibition was obtained at 10 μM PREG, with no statistical difference between 10 and 100 μM PREG, which account for 24.3±0.95% and 30.5±0.85% inhibition of pre-drug BK activity, respectively (Fig. 5B–C). PREG action had an EC_{50}=1 μM which resulted in 8.79±0.97% reduction in pre-drug BK activity (Fig 5C; reduced Chi-square=0.13, R-square=0.99). At all concentrations, PREG action on excised patches were fully washable with control perfusion (Fig. 5B). Thus, the concentration-

dependent inhibition of BK channels in cell-free myocyte membranes by PREG (Fig. 5) closely followed the concentration-dependent arterial constriction (whether *in vitro* or *in vivo)* by this neurosteroid (Figs. 1–2). Taken together with the fact that PREG-induced constriction of de-endothelialized MCA was removed by the BK channel inhibitor paxilline (Fig. 3), our patch-clamp data indicate that the main target of PREG vasoconstriction is the SM BK complex. Moreover, inhibition of BK currents in cell-free membrane patches indicates that this action does not require cell integrity, organelles or the continuous presence of cytosolic signals. Rather, BK themselves and their immediate proteolipid environment suffice to mediate PREG action.

3.5 BK inhibition by PREG is mediated through the channel-forming α (slo1) subunit.

Incerebral artery SM, BK channel complexes include channel-forming α subunits and auxiliary subunits of β_1 and gamma types (Brenner et al., 2000; Evanson et al., 2014; Dopico et al., 2018), yet β_1 is critical for determining the channel physiological phenotype and its response to some physiological steroids including cholanes (Bukiya et al., 2013) and 17β-estradiol (Granados et al., 2019). Thus, to determine whether β_1 subunits were necessary for or modified the inhibitory actions by PREG on native SM BK channels, we evaluated the effect of 10 μM PREG in I/O patches of SM myocytes freshly isolated from MCAs of male *KCNMB1*$^{-/-}$ mice (Fig. 6). DMSO time-matched perfusions did not differ between patches from MCAs of *KCNMB1*$^{-/-}$ mice when compared to their *wt* counterparts (background strain C57BL/6) (Fig. 6B–C). BK current inhibition elicited by bath perfusion of 10 μM PREG to I/O patches did not significantly differ between wt (C57BL/6J) and *KCNMB1*$^{-/-}$ mice: 24.3±0.95% and 60.8±0.81% of pre-drug levels, respectively (Fig. 6). These data document that β_1 neither is required for nor significantly regulates PREG inhibitory action on BK currents and, thus, is not a primary target of PREG.

In order to investigate the potential involvement of the proteolipid environment (including gamma auxiliary subunit) in PREG-induced inhibition of cerebrovascular BK current, we reconstituted BK channel–forming slo1 subunits cloned from cerebral artery myocytes (cbv1, Jaggar et al., 2005) into binary phospholipid planar bilayers (POPE/POPS 3:1 w/w), with *trans* and *cis* solutions containing 30 μM free [Ca^{2+}]. PREG stock dissolved in DMSO or the equivalent amount DMSO was added to both the *cis* and *trans* solution after protein incorporation and recording of basal activity of the channels for 2 minutes, to reach a final concentration of 10 μM. Addition of DMSO or PREG to both solutions ensured that concentrations remained constant and did not become diluted through inevitable passive diffusion through the bilayer membrane. PREG (10 μM) significantly inhibited BK activity when compared to its time- and concentration-matched DMSO control with a maximum effect of 66.1±0.93% of basal activity being recorded immediately before addition the neurosteroid (Fig. 7). Moreover, PREG-driven inhibition of BK activity in artificial lipid bilayers was similar to that found in I/O patches of *KCNMB1*$^{-/-}$ mouse myocytes (Fig. 7C vs. 6C). Thus, the complex proteolipid environment typical of native SM membranes, which could include BK γ subunits, is not needed for PREG to inhibit cerebrovascular BK activity. Rather, the BK channel-forming α (slo1) subunit within a bare phosphoglyceride environment suffices.

Finally, to establish that slo1 proteins ultimately mediate PREG-induced brain artery constriction, 10 μM PREG was applied to de-endothelialized MCAs from male and female *KCNMA1*$^{-/-}$ mice (Fig. 8). As expected, 10 μM PREG application resulted in a very mild dilation of both male and female *KCNMA1*$^{-/-}$ MCAs (Fig. 8). This dilation was significantly different when compared to the combined application of PREG and the steroid blockers (20 μM ketoconazole) to block PXR, 33 μM MK-886 to block PPAR, and 20 μM MFA to block TRPM3) (Fig. 8B, D; P=0.0125, P=0.0121 for male and female mouse arteries, respectively; Mann Whitney U-test). Moreover, the constriction caused by the application of the steroid blockers alone significantly differed from the lack of response in the combined application of PREG and the steroid blockers (Fig. 8C/D P=0.0119, P=0.0121 for male and female mouse arteries, respectively; Mann Whitney U-test). Thus, our data suggest that the very mild dilation evoked by 10 μM PREG on male and female *KCNMA1*$^{-/-}$ mice may be attributed to PREG targets other than BK channels. i.e., membrane receptors well-known to be targeted by this neurosteroid. In sharp contrast, the significant vasoconstriction elicited by PREG in wild-type mice, whether male or female, is due to direct sensing of PREG by the BK α subunits.

4.1 Discussion

Our study demonstrates for the first time that PREG constricts brain arteries *in vivo* and *in vitro.* To prove this, we respectively used cranial windows on pial arteries branching out from the MCA and pressurized, isolated MCA segments. These two systems have been widely used to study cerebral artery physiology, pathology, and pharmacology (Asscheman et al., 2014; Basar et al., 2005; Cutler and Laue, 1990; Plüger et al., 2000; Tano and Gallasch, 2014). Moreover, the mouse cerebral circulation greatly matches that of humans (Lee, 1995). We chose MCA because: 1-MCA perfuses more brain territories than the other branches of Willis' circle (Lee, 1995; Lehecka et al., 2012); 2-MCA tone and diameter modifications are associated with numerous cerebrovascular, including ischemic, disorders (Cipolla and Curry, 2002; González Delgado and Bogousslavsky, 2012; Krafft et al., 2012); 3-MCA has been used in our previous studies of ethanol-induced constriction of cerebral arteries and its mediation by SM BK channels (Bukiya et al., 2009; Liu et al., 2004), as well as to demonstrate the key role of these K^+ channels as effectors of drug-induced cerebrovascular dilation (Bukiya et al., 2007; Bukiya et al., 2013). The magnitude of PREG effect on MCA diameter reported in the present study is considered as a robust constriction, with a maximal decrease in diameter of ~35 and 25% over pre-drug values for male and female, respectively. Poiseuille's law (Rushmer, 1972) establishes that flow is related to vessel radius by a power of 4; thus, our results indicate that PREG at E_{max} would evoke a drastic decrease in local CBF, even more robust than what is seen in ischemic events (Cipolla and Curry, 2002; González Delgado and Bogousslavsky, 2012).

BK-channel forming slo1 proteins are expressed in significant amounts in many cerebral arteries, thus suggesting that PREG should have constricting properties in cerebral arteries other than MCA (Kuntamallappanavar et al., 2017). The similarities in PREG-induced constriction of MCA *in vivo* (Fig. 1) and *in vitro* (Fig. 2), indicates that PREG systemic metabolism, circulating factors or any possible interactions with the anesthetic agents do not significantly affect the neurosteroid-induced cerebral vasoconstriction. PREG-induced

constriction of cerebral arteries is also endothelium-independent. This becomes particularly important in clinical cases where the endothelium function declines, such as drug abuse, obesity, and natural progression of ageing (Berg et al., 1998; Hunter et al., 2012; Villella and Cho, 2015). It is important to note that PREG is under investigation for the treatment of benzodiazepine, cannabis and drug abuse, and the alleviation of withdrawal-induced anxiety disorders, as well as drug-induced psychotic-like states (Busquets-Garcia et al., 2017; Reddy and Kulkarni, 1997; Tomaselli and Vallée, 2019; Vallée et al., 2014). Clinical studies involving PREG therapy (up to 500 mg/day for 8 weeks) consistently document several-fold increases in PREG serum levels posttreatment (Brown et al., 2014; Marx et al, 2009). While safe levels of PREG beyond a 12-week period are not known, it should be noted that: 1-serum PREG levels do reach sub-μM levels (Brown et al., 2014; Marx et al, 2009); 2-in general, brain steroid levels exceed circulating levels because of an accumulation of the steroid by brain tissues and/or contribution by local synthesis (Kanchevaa et al., 2011; Wang et al., 1997); 3-steroid concentrations in the brain may be further influenced by circulating hormones. Thus, females may be at a greater risk to PREG therapy side-effects (Kanchevaa et al., 2011; Wang et al., 1997). In addition, while circulating levels of PREG during therapy increase several-fold and reach sub-μM levels, circulating levels of PREG sulfate is a more accurate indicator of PREG levels within the brain, which are higher than those in systemic circulation (Baulieu et al., 2001; Brown et al., 2014; Kanchevaa et al., 2011). Collectively, data from our studies documenting BK channel-mediated MCA constriction at sub-μM to μM levels of PREG strongly suggest that the aforementioned treatments with PREG could pose potential associated risks, due to PREG-induced cerebral artery constriction. Because cognition and other cerebral functions vitally depend on adequate blood perfusion, eventually determined by the diameter of resistance size cerebral arteries (Cox and Rusch, 2002; Jackson, 2005; Moudgil et al., 2006), the possible therapeutic properties being investigated for PREG in cognitive function and Alzheimer's could be negatively affected by the cerebral constriction seen at higher concentrations (Akan et al., 2008; Akwa, 2020; Fung et al., 2014; Lejri et al., 2019; Masuyama et al., 2016; Mayo et al., 2003, 2005).

Collectively, our current study shows that slo1 subunits suffice to evoke PREG inhibition of BK activity and mediate the brain artery constriction evoked by this neurosteroid. Based on the wt and *KCNMA1*$^{-/-}$ MCA responses to PREG in presence of selective blockers, we can also advance that other known targets of PREG, such as G-coupled steroid receptors, do not primarily contribute to PREG-induced cerebrovascular constriction. Rather, they mediated a mild dilation in response to PREG (Fig. 3, Fig 8), which was unmasked when the *KCNMA*$^{-/-}$ gene was fully knock-down. This suggests that even though PREG may interact with PXR, PPAR and TRPM3, the overriding factor in PREG-induced brain artery constriction is BK inhibition. Despite the involvement of this common target of PREG in male and female animals, it is important to note that the overall responses to lower concentrations of PREG (≤10 μM) differ between male and female mice (Supplemental Fig. 1). Indeed, males are more susceptible to PREG-induced constriction in intact and de-endothelialized MCA's at 1 μM PREG and to 10 μM PREG in de-endothelialized vessels, when compared to females (Supplemental Fig. 1A; P=0.0119, P=0.0079, P=0.079, respectively). This difference seems to be driven not only by a difference in overall BK-induced effects, but also by steroid receptor-mediated effects; female mice have a larger protective vasodilatory response from

steroid receptors and less constriction associated with the BK-mediated response (Supplemental Fig. 1B; P=0.0079, P=0.0086, respectively). This difference could be due to a difference in concentration of these receptors in the SM. Finally, the fact that PREG cerebral artery constriction is totally lost in presence of combined BK and steroid receptors blockers indicate that “third-parties” that could mediate endothelial-independent cerebral artery constriction (e.g. TRPV1; North et al., 2018) do not play a role in the overall PREG-induced responses in males or females.

Lastly, our study unequivocally demonstrates that the auxiliary subunits commonly associated with BK in SM membranes are neither necessary for nor significantly modulate PREG-induced inhibition of BKs: PREG produced a robust inhibition of native channel activity in *KCNMB1*$^{-/-}$ mice. It could be argued, however, that in addition to β_1 subunits, auxilliary γ subunits still present in *KCNMB1*$^{-/-}$ cerebrovascular myocytes (Evanson et al., 2014) could contribute to PREG effect on BK function. This possibility, however, is highly unlikely: direct application of PREG at E_{max} (10 μM) to homomeric slo1 (cbv1 isoform) channels reconstituted into artificial lipid bilayers produced a maximum average reduction in NPo, which was comparatively similar to the inhibition evoked by equal concentrations of PREG in native BKs from excised membrane patches of wt and *KCNMB1*$^{-/-}$ (Figs. 5–7). We cannot rule out that some γ subunits could incorporate into bilayers and form functional complexes with cbv1. However, the large difference in molecular weight of these proteins (35 kDa for γ subunit versus ~130 kDa for slo1) is very likely to preclude their concomitant presence within the same layer of sucrose gradient used for protein preparation for bilayer experiments (Zhang and Yan, 2014). In addition, to our knowledge, CHO cells here used to make the bilayer preparation have not been reported to express any of the major types of BK γ subunits (Yan and Aldrich, 2012; Zhang and Yan, 2014). Therefore, it is reasonable to conclude that only the channel-forming α (slo1; cbv1) subunit is necessary for the PREG-induced inhibition of BK.

While our study conclusively demonstrates that slo1 proteins in a binary phospholipid bilayer behave as molecular sensors of PREG inhibition of BK function, whether these subunits provide actual recognition sites for the neurosteroid remains to be studied. From a historical perspective, the interactions of PREG with BK channels can be analyzed by two distinct theories that have previously been applied to cholesterol (Dopico et al., 2012; Bukiya and Dopico, 2019), which is PREG main precursor in the body. The first is the “lipid theory”, which indicates that cholesterol modification of BK function results as a consequence of steroid insertion into the lipid bilayer with consequent modification of bilayer physical properties and thus, BK conformation and function. The second is the “protein theory”, which proposes that cholesterol-induced modification of BK function results from initial binding of the steroid to the BK subunits themselves, with or without secondary modifications in bilayer lipid properties. Steroids like cholesterol are well-known to embed into the lipid bilayer of cell membranes and thus affect several physical properties of the bulk bilayer, including broadening of the gel-to-liquid crystalline phase transition, decrease in the cross sectional area occupied by the phospholipid in the liquid-crystalline state, increase in lateral stress and stiffness of the phospholipid monolayer or bilayer in the physiologically relevant fluid phase, increase in the modulus of compressibility and mechanical strength, introduction of negative monolayer curvature and increase in bilayer

thickness, and modification of the bilayer electrical dipole in a nonmonotonic fashion (reviewed in Dopico et al., 2012; Dopico et al., 2020). In turn, these modifications can alter ion channel (including BK) function (Lundbæk, 2008; Dopico et al., 2012; 2020; Ayee and Levitan, 2016). Remarkably, the PREG molecule shares many of the chemical properties of cholesterol, and is subject to passive, lipophilicity-driven accumulation in cell membranes (McManus et al., 2019). Moreover, simulation data indicate that PREG inserts into phospholipid bilayers as cholesterol does (Atkovska et al., 2018). Thus, it is possible to speculate that sub-μM to μM PREG, as used in our study, could result in membrane PREG molar fractions sufficient to alter the bilayer properties known to be modified by cholesterol and, eventually, alter BK channel function. On the other hand, cholesterol has been shown to interact directly with the BK channel-forming subunit, leading to decreased channel activity (Dopico et al., 2012; Bukiya and Dopico, 2019). Based on the chemical and structural similarities between PREG and cholesterol, one could also hypothesize that PREG directly interacts with BK α subunits at their cholesterol-sensing regions. While these the “lipid” and “protein” interpretations have been traditionally presented as mutually exclusive, there is no reason to downplay the possibility of their concomitant contribution to steroid, whether cholesterol or PREG, effects on BK function.

In conclusion, we have shown for the first time that PREG at concentrations reached in the brain during physiology or pharmaco-therapeutics (PREG supplements) constricts cerebral arteries of both male and females in a reversibly and concentration-dependent manner, and independently of circulating, paracrine, neuronal, glial, and endothelial factors. PREG-induced constriction of brain arteries is due to the inhibition of BK channels found within the cerebrovascular SM itself. This action is possible through PREG-sensing by the channel-forming slo1 proteins. Thus, our work, which spans from organismal to molecular resolution, provides new insights on the biological effects of PREG, allowing for a better understanding of the effects of PREG and its derivatives when used to treat prevalent brain disorders.

Supplementary Material

Refer to Web version on PubMed Central for supplementary material.

Acknowledgements.

Authors very much thank Professor Andrea Meredith (University of Maryland) for her generous gift of *KCNMA1*$^{-/-}$ mice. We also deeply thank Alexandria Slayden for her technical assistance in cell culture, mouse surgeries, and transfections.

This work was supported by the National Institute on Alcohol Abuse and Alcoholism (Grant R37-AA11560; AMD) and the National Heart, Lung, and Blood Institute (Grant R01-HL-147315; AMD).

Abbreviations.

BK	calcium- and voltage-gated potassium channel of large conductance
CBF	cerebral blood flow
CHO cells	Chinese hamster ovary cells

DMSO	dimethyl sulfoxide
MCA	middle cerebral artery
POPE	1-palmitoyl-2-oleoyl-*sn*-glycero-3-phosphoethanolamine
POPS	1-palmitoyl-2-oleoyl-*sn*-glycero-3-phospho-L-serine (sodium salt)
PPAR	peroxisome proliferator-activated receptor
PREG	pregnenolone, PSS: physiologic sodium saline
PXR	pregnane X receptor
slo1	*CBV1*-AY330293
SM	smooth muscle
TRPM3	transient receptor potential cation channel subfamily M member 3

6.1 References

Akan P, Kizildag S, Ormen M, Genc S, Oktem MA, Fadiloglu M, 2009. Pregnenolone protects the PC-12 cell line against amyloid p peptide toxicity but its sulfate ester does not. Chem. Biol. Interact 177:65–70. DOI: 10.1016/j.cbi.2008.09.016. [PubMed: 18926803]

Akwa Y, 2020. Steroids and Alzheimer's Disease: Changes Associated with Pathology and Therapeutic Potential. Int J Mol Sci. 21(13): 4812. DOI: 10.3390/ijms21134812.

Amberg GC, Santana LF, 2003. Downregulation of the BK channel beta1 subunit in genetic hypertension. Circ Res. 93(10):965–971. DOI: 10.1161/01.RES.0000100068.43006.36. [PubMed: 14551242]

Antollini SS, Barrantes FJ, 2016. Fatty Acid Regulation of Voltage- and Ligand-Gated Ion Channel Function. Front Physiol. 7:573. DOI: 10.3389/fphys.2016.00573. [PubMed: 27965583]

Asscheman H, T'Sjoen G, Lemaire A, Mas M, Meriggiola MC, Mueller A, Kuhn A, Dhejne C, Morel-Journel N, Gooren JL, 2014. Venous thrombo-embolism as a complication of cross-sex hormone treatment of male-to-female transsexual subjects: a review. Andrologia. 46(7):791–5. DOI: 10.1111/and.12150. [PubMed: 23944849]

Atkovska K, Klingler J, Oberwinkler J, Keller S, Hub JS, 2018. Rationalizing Steroid Interactions with Lipid Membranes: Conformations, Partitioning, and Kinetics. ACS Cent Sci. 4(9):1155–1165. DOI:10.1021/acscentsci.8b00332. [PubMed: 30276248]

Ayee MA, Levitan I, 2016. Paradoxical impact of cholesterol on lipid packing and cell stiffness. Front Biosci (Landmark Ed). 21:1245–59. DOI: 10.2741/4454. [PubMed: 27100504]

Basar MM, Aydin G, Mert HC, Keles I, Caglayan O, Orkun S, Batislam E, 2005. Relationship between serum sex steroids and Aging Male Symptoms score and International Index of Erectile Function. Urology 66:597–601. DOI: 10.1016/j.urology.2005.03.060. [PubMed: 16140085]

Baulieua EE, Robela P, Schumachera M, 2001. Neurosteroids: Beginning of the story. International Review of Neurobiology. 46:1–32. DOI: 10.1016/S0074-7742(01)46057-0. [PubMed: 11599297]

Baumbach GL, Heistad DD, 1985. Regional, segmental, and temporal heterogeneity of cerebral vascular autoregulation. Ann Biomed Eng.13:303–10. DOI: 10.1007/BF02584248. [PubMed: 3898928]

Berg L, McKeel DW Jr., Miller JP, Storandt M, Rubin EH, Morris JC, Baty J, Coats M, Norton J, Goate AM, Price JL, Gearing M, Mirra SS, Saunders AM, 1998. Clinicopathologic studies in cognitively healthy aging and Alzheimer's disease: relation of histologic markers to dementia severity, age, sex, and apolipoprotein E genotype. Arch. Neurol. 55:326–35. DOI: 10.1001/archneur.55.3.326. [PubMed: 9520006]

Brayden JE, Nelson MT, 1992. Regulation of arterial tone by activation of calcium-dependent potassium channels. Science. 256(5056):532–5. DOI: 10.1126/science.1373909. [PubMed: 1373909]

Brenner R, Perez GJ, Bonev AD, Eckman DM, Kosek JC, Wiler SW, Patterson AJ, Nelson MT, and Aldrich RW, 2000. Vasoregulation by the beta1 subunit of the calcium-activated potassium channel. Nature 407:870–876. DOI: 10.1038/35038011. [PubMed: 11057658]

Brown ES, Park J, Marx CE, Hynan LS, Gardner C, Davila D, Nakamura A, Sunderajan P, Lo A, Holmes T, 2014. A randomized, double-blind, placebo-controlled trial of pregnenolone for bipolar depression. Neuropsychopharmacology: official publication of the American College of Neuropsychopharmacology. 39(12), 2867–2873. DOI: 10.1038/npp.2014.138. [PubMed: 24917198]

Bukiya AN, Belani JD, Rychnovsky S, Dopico AM, 2011a. Specificity of cholesterol and analogs to modulate BK channels points to direct sterol-channel protein interactions. J Gen Physiol 137: 93–110. DOI: 10.1016/j.pharmthera.2012.05.002 [PubMed: 21149543]

Bukiya AN, Dopico AM, 2019. Regulation of BK Channel activity by cholesterol and its derivatives. Adv Exp Med Biol. 1115:53–75. DOI: 10.1007/978-3-030-04278-3_3. [PubMed: 30649755]

Bukiya AN, Kuntamallappanavar G, Edwards J, Singh AK, Shivakumar B, Dopico AM, 2014. An alcohol-sensing site in the calcium- and voltage-gated, large conductance potassium (BK) channel. Proc Natl Acad Sci U S A. 111(25):9313–8. DOI: 10.1073/pnas.1317363111. [PubMed: 24927535]

Bukiya AN, Liu J, Dopico AM, 2009. The BK channel accessory beta1 subunit determines alcohol-induced cerebrovascular constriction. FEBS letters 583:2779–2784. DOI: 10.1016/j.febslet.2009.07.019. [PubMed: 19616547]

Bukiya AN, Liu J, Toro L, Dopico AM, 2007. Beta1 (KCNMB1) subunits mediate lithocholate activation of large-conductance Ca2+ -activated K+ channels and dilation in small, resistance-size arteries. Mol Pharmacol 72: 359–369. DOI: 10.1124/mol.107.034330. [PubMed: 17468198]

Bukiya AN, McMillan JE, Fedinec AL, Patil SA, Miller DD, Leffler CW, Parrill AL, Dopico AM, 2013. Cerebrovascular dilation via selective targeting of the cholane steroid recognition site in the BK channel pi-subunit by a novel nonsteroidal agent. Mol Pharmacol 83: 1030–1044. DOI: 10.1124/mol.112.083519. [PubMed: 23455312]

Bukiya AN, Vaithianathan T, Kuntamallappanavar G, Asuncion-Chin M, Dopico AM, 2011b. Smooth muscle cholesterol enables BK pi subunit-mediated channel inhibition and subsequent vasoconstriction evoked by alcohol. Arterioscler Thromb Vasc Biol 31: 2410–2423. DOI: 10.1161/ATVBAHA.111.233965. [PubMed: 21868700]

Busija DW, Leffler CW, 1991. Selective attenuation by perivascular blood of prostanoid-dependent cerebrovascular dilation in piglets. Stroke: 22:484–488. DOI: 10.1161/01.str.22.4.484. [PubMed: 1902599]

Busquets-Garcia A, Soria-Gómez E, Redon B, Mackenbach Y, Vallée M, Chaouloff F, Varilh M, Ferreira G, Piazza PV, Marsicano G, 2017. Pregnenolone blocks cannabinoid-induced acute psychotic-like states in mice. Mol Psychiatry. 22(11):1594–1603. DOI: 10.1038/mp.2017.4. [PubMed: 28220044]

Chang HM, Reitstetter R, Mason RP, Gruener R, 1995. Attenuation of channel kinetics and conductance by cholesterol: an interpretation using structural stress as a unifying concept. J Membr Biol. 143:51–63. DOI: 10.1007/BF00232523. [PubMed: 7714888]

Cipolla MJ, Curry AB, 2002. Middle cerebral artery function after stroke: the threshold duration of reperfusion for myogenic activity. Stroke. 33:2094–2099. DOI: 10.1161/01.str.0000020712.84444.8d. [PubMed: 12154269]

Cox RH, Rusch NJ, 2002. New expression profiles of voltage-gated ion channels in arteries exposed to high blood pressure. Microcirculation. 9:243–257. DOI: 10.1038/sj.mn.7800140. [PubMed: 12152102]

Crowley JJ, Treistman SN, Dopico AM, 2003. Cholesterol antagonizes ethanol potentiation of human brain BKCa channels reconstituted into phospholipid bilayers. Mol Pharmacol 64:365–372. DOI: 10.1124/mol.64.2.365. [PubMed: 12869641]

Cutler GB Jr., Laue L, 1990. Congenital adrenal hyperplasia due to 21-hydroxylase deficiency. N Engl J Med. 323(26):1806–13. DOI: 10.1210/edrv.21.3.0398. [PubMed: 2247119]

Dopico AM, Bukiya AN, 2014. Lipid regulation of BK channel function. Front Physiol. 5:312. DOI: 10.3389/fphys.2014.00312. [PubMed: 25202277]

Dopico AM, Bukiya AN, Jaggar JH, 2018. Calcium- and voltage-gated BK channels in vascular smooth muscle. Pflugers Arch. 470(9):1271–1289. DOI: 10.1007/s00424-018-2151-y. [PubMed: 29748711]

Dopico AM, Bukiya AN, North K, 2020. Cholesterol modulation of BK (MaxiK; Slo1) Channels. New Techniques for Studying Biomembranes. Qiu-Xing Jiang. (7–22). Taylor and Francis.

Dopico AM, Bukiya AN, Singh AK, 2012. Large conductance, calcium- and voltage-gated potassium (BK) channels: regulation by cholesterol. Pharmacol Ther 135: 133–50. DOI: 10.1016/j.pharmthera.2012.05.002. [PubMed: 22584144]

Evanson KW, Bannister JP, Leo MD, Jaggar JH, 2014. LRRC26 is a functional BK channel auxiliary γ subunit in arterial smooth muscle cells. Circ Res: 115(4):423–341. DOI: 10.1161/CIRCRESAHA.115.303407 [PubMed: 24906643]

Faraci FM, Sobey CG, 1998. Role of Potassium Channels in Regulation of Cerebral Vascular Tone. J Cereb Blood Flow Metab. 18(10):1047–1063. DOI: 10.1097/00004647-199810000-00001. [PubMed: 9778181]

Figueroa-Valverde L, Diaz-Cedillo F, Diaz-Ku E, Camacho-Luis A, 2009. Effect induced by hemisuccinate of pregnenolone on perfusion pressure and vascular resistance in isolated rat heart. African J of Pharm. 234–241. DOI: 10.5897/AJPP.9000102.

Figueroa-Valverde L, Diaz-Cedillo F, Garcia-Cervera E, Pool-Gomez E, Lopez-Ramos M, Sarabia-Alcocer B, Rosas-Nexticapa M, Mendoza-Lopez R, 2014. Antimicrobial Activity Induced by A Steroid-brucine Derivative on S. typhi, K. pneumoniae and E. coli. Journal of Bio Sci.14(1):67–72. DOI: jbs.2014.67.72.

Finn DA, Ford MM, Wiren KM, Roselli CE, Crabbe JC, 2004. The role of pregnane neurosteroids in ethanol withdrawal: behavioral genetic approaches. Pharmacol Ther. 101(2):91–112. DOI: 10.1016/j.pharmthera.2003.10.006. [PubMed: 14761701]

Freedman DA, 2009. Statistical Models: Theory and Practice. Cambridge University Press. ISBN 978–1-139–47731-4.

Fung LK, Libove RA, Phillips J, Haddad F, Hardan AY, 2014. Brief report: an open-label study of the neurosteroid pregnenolone in adults with autism spectrum disorder. J Autism Dev Disord. 44(11):2971–7. DOI: 10.1007/s10803-014-2144-4. [PubMed: 24849255]

González Delgado M, Bogousslavsky J, 2012. Superficial Middle Cerebral Artery Territory Infarction: Manifestations of Stroke. Front Neurol Neurosci. Basel, Karger, vol 30, pp 111–114. DOI: 10.1159/000333604.

Granados ST, Castillo K, Bravo-Moraga F, Sepúlveda RV, Carrasquel-Ursulaez W, Rojas M, Carmona E, Lorenzo-Ceballos Y, González-Nilo F, González C, Latorre R, Torres YP, 2019. The molecular nature of the 17p-Estradiol binding site in the voltage- and Ca 2+-activated K + (BK) channel pi subunit. Sci Reports. 9(1):9965. DOI: 10.1038/s41598-019-45942-1.

Hunter JM, Kwan J, Malek-Ahmadi M, Maarouf CL, Kokjohn TA, Belden C, Sabbagh MN, Beach TG, Roher AE, 2012. Morphological and pathological evolution of the brain microcirculation in aging and Alzheimer's disease. PloS one. 7(5):e36893. DOI: 10.1371/journal.pone.0036893. [PubMed: 22615835]

Jackson WF, 2005. Potassium channels in the peripheral microcirculation. Microcirculation. 12:113–127. DOI: 10.1080/10739680590896072. [PubMed: 15804979]

Jaggar JH, Li A, Parfenova H, Liu J, Umstot ES, Dopico AM, Leffler CW, 2005. Heme Is a Carbon Monoxide Receptor for Large-Conductance Ca2+-Activated K+ Channels. Circulation Research. 97:805–812. DOI: 10.1161/01. [PubMed: 16166559]

Kanchevaa R, Hilla M, Novákb Z, Chrastinab J, Kanchevaa L, Stárkaa L, 2011. Neuroactive steroids in periphery and cerebrospinal fluid. Neuroscience. 191: 22–27. DOI: 10.1016/j.neuroscience.2011.05.054. [PubMed: 21641969]

Krafft PR, Bailey EL, Lekic T, Rolland WB, Altay O, Tang J, Wardlaw JM, Zhang JH, Sudlow CL, 2012. Etiology of stroke and choice of models. Int J Stroke. 7:398–406. DOI: 10.1111/j.1747-4949.2012.00838.x. [PubMed: 22712741]

Kublickiene K, Luksha L, 2008. Gender and the endothelium. Pharmacol Rep. 60(1):49–60. [PubMed: 18276985]

Kuntamallappanavar G, Bisen S, Bukiya AN, Dopico AM, 2017. Differential distribution and functional impact of BK channel beta1 subunits across mesenteric, coronary, and different cerebral arteries of the rat. Pflugers Arch. 469(2):263–277. DOI: 10.1007/s00424-016-1929-z. [PubMed: 28012000]

Kuntamallappanavar G, Toro L, Dopico AM, 2014. Both transmembrane domains of BK β1 subunits are essential to confer the normal phenotype of β1-containing BK channels. PLoS One. 9(10):e109306. DOI: 10.1371/journal.pone.0109306. [PubMed: 25275635]

Latorre R, Castillo K, Carrasquel-Ursulaez W, Sepulveda RV, Gonzalez-Nilo F, Gonzalez C, Alvarez O, 2017. Molecular Determinants of BK Channel Functional Diversity and Functioning. Physio Rev. 97(1):39–87. DOI: 10.1152/physrev.00001.2016.

Lee RM 1995. Morphology of cerebral arteries. Pharmacol Ther. 66(1):149–73. DOI: 10.1016/0163-7258(94)00071-a. [PubMed: 7630927]

Lee E, Grodzinsky AJ, Libby P, Clinton SK, Lark MW, Lee RT 1995. Human vascular smooth muscle cellmonocyte interactions and metalloproteinase secretion in culture. Arterioscler. Thromb. Vasc. Biol.15:2284–2289. DOI: 10.1161/01.ATV.15.12.2284. [PubMed: 7489254]

Lehecka M, Dashti R, Rinne J, Romani R, Kivisaari R, Niemelä M, Hernesniemi J, 2012. Surgical management of aneurysms of the middle cerebral artery. Schmidek and Sweet Operative Neurosurgical Techniques, 6th Edition. Saunders, Cambridge, MA. Pp. 897913. DOI: 10.1016/0090-3019(95)80032-c.

Lejri I, Grimm A, Halle F, Abarghaz M, Klein C, Maitre M, Schmitt M, Bourguignon JJ, Mensah-Nyagan AG, Bihel F, Eckert A, 2019. TSPO Ligands Boost Mitochondrial Function and Pregnenolone Synthesis. J. Alzheimers Dis. 72:1045–1058. DOI: 10.3233/JAD-190127. [PubMed: 31256132]

Li Q, Yan J, 2016. Modulation of BK Channel Function by Auxiliary Beta and Gamma Subunits. Int Rev Neurobiol. 128:51–90. DOI: 10.1016/bs.irn.2016.03.015. [PubMed: 27238261]

Liu P, Xi Q, Ahmed A, Jaggar JH, Dopico AM, 2004. Essential role for smooth muscle BK channels in alcohol-induced cerebrovascular constriction. Proc Natl Acad Sci U S A 101: 18217–18222. DOI: 10.1073/pnas.0406096102. [PubMed: 15604147]

Lundbæk AJ, 2008. Lipid Bilayer-mediated Regulation of Ion Channel Function by Amphiphilic Drugs. J Gen Physiol. 131 (5): 421–429. DOI: 10.1085/jgp.200709948. [PubMed: 18411332]

Marx CE, Keefe RS, Buchanan RW, Hamer RM, Kilts JD, Bradford DW, Strauss JL, Naylor JC, Payne VM, Lieberman JA, Savitz AJ, Leimone LA, Dunn L, Porcu P, Morrow AL, Shampine LJ, 2009. Proof-of-concept trial with the neurosteroid pregnenolone targeting cognitive and negative symptoms in schizophrenia. Neuropsychopharmacology. 34(8):1885–1903. DOI: 10.1038/npp.2009.26. [PubMed: 19339966]

Masuyama H, Nakamura K, Nobumoto E, Hiramatsu Y, 2016. Inhibition of pregnane X receptor pathway contributes to the cell growth inhibition and apoptosis of anticancer agents in ovarian cancer cells. Int J Oncol. 49:3(1211–1220). DOI: 10.3892/ijo.2016.3611. [PubMed: 27572875]

Mayo W, George O, Darbra S, 2003. Individual differences in cognitive aging: implication of pregnenolone sulfate. Prog Neurobiol. 71(1):43–8. DOI: 10.1016/j.pneurobio.2003.09.006. [PubMed: 14611866]

Mayo W, Lemaire V, Malaterre J, 2005. Pregnenolone sulfate enhances neurogenesis and PSA-NCAM in young and aged hippocampus. Neurobio Aging. 26:1(103–114). DOI: 10.1016/j.neurobiolaging.2004.03.013.

McCurley A, McGraw A, Pruthi D, Jaffe IZ, 2013. Smooth muscle cell mineralocorticoid receptors: role in vascular function and contribution to cardiovascular disease. Pflugers Arch. 465(12):1661–70. DOI: 10.1007/s00424-013-1282-4. [PubMed: 23636772]

McManus JM, Bohn K, Alyamani M, Chung YM, Klein EA, Sharifi N. Rapid and structure-specific cellular uptake of selected steroids. PLoS One. 2019 10 17;14(10):e0224081. doi: 10.1371/journal.pone.0224081. eCollection 2019. [PubMed: 31622417]

Moudgil R, Michelakis ED, Archer SL, 2006. The role of K+ channels in determining pulmonary vascular tone, oxygen sensing, cell proliferation, and apoptosis: implications in hypoxic pulmonary vasoconstriction and pulmonary arterial hypertension. Microcirculation 13:615–32. DOI: 10.1080/10739680600930222. [PubMed: 17085423]

Navarro-Orozco D, Sánchez-Manso JC, 2020. Neuroanatomy, Middle Cerebral Artery. In: StatPearls [Internet]. Treasure Island (FL): StatPearls Publishing.

North K, Chang J, Bukiya AN, Dopico AM, 2018. Extra-endothelial TRPV1 channels participate in alcohol and caffeine actions on cerebral artery diameter. Alcohol. 73:45–55. DOI: 10.1016/j.alcohol.2018.04.002. [PubMed: 30268908]

North K, Slayden A, Mysiewicz S, Bukiya A, Dopico A, 2020. Celastrol Dilates and Counteracts Ethanol-Induced Constriction of Cerebral Arteries. J Pharmacol Exp Ther. 375(2):247–257. DOI: 10.1124/jpet.120.000152. [PubMed: 32862144]

Oren I, 2004. Free diffusion of steroid hormones across biomembranes: A simplex search with implicit solvent model calculations. Biophysical Journal. 87 (2): 768–79. DOI: 10.1529/biophysj.103.035527. [PubMed: 15298886]

Orio P, Rojas P, Ferreira G, Latorre R, 2002. New disguises for an old channel: MaxiK channel b-subunits. News Physiol Sci 17:156–161. DOI: 10.1152/nips.01387.2002. [PubMed: 12136044]

Pérez GJ, Bonev AD, Nelson MT, 2001. Micromolar Ca(2+) from sparks activates Ca(2+)- sensitive K(+) channels in rat cerebral artery smooth muscle. Am J Physiol Cell Physiol 281: C1769–C1775. DOI: 10.1152/ajpcell.2001.281.6.C1769. [PubMed: 11698234]

Porcu O, Morrow AL, 2014. Divergent neuroactive steroid responses to stress and ethanol in rat and mouse strains: relevance for human studies. Psychopharmacology (Berl). 231(17):3257–72. DOI: 10.1007/s00213-014-3564-8. [PubMed: 24770626]

Plüger S, Faulhaber J, Fürstenau M, Löhn M, Waldschütz R, Gollasch M, Haller H, Luft FC, Ehmke H, Pongs O, 2000. Mice with disrupted BK channel beta1 subunit gene feature abnormal Ca2+ spark/STOC coupling and elevated blood pressure. Circ Res. 87:E53–E60. DOI: 10.1161/01.res.87.11.e53. [PubMed: 11090555]

Reddy DS, Kulkarni SK, 1997. Neurosteroid coadministration prevents development of tolerance and augments recovery from benzodiazepine withdrawal anxiety and hyperactivity in mice. Methods Exp Clin Pharmacol. 19(6):395–405.

Rizvi YQ, Mehta CS, Oyekan A, 2013. Interactions of PPAR-alpha and adenosine receptors in hypoxia-induced angiogenesis. Vascul Pharmacol. 59:144–51. DOI: 10.1016/j.vph.2013.09.001. [PubMed: 24050945]

Rushmer RF 1972. Organ Physiology: structure and function of the. cardiovascular system. Saunders : Philadelphia, 1972; 135. DOI: 10.7326/0003-4819-77-2-334_1.

Singh AK, McMillan J, Bukiya AN, Burton B, Parrill AL, Dopico AM, 2012. Multiple cholesterol recognition/interaction amino acid consensus (CRAC) motifs in cytosolic C tail of Slo1 subunit determine cholesterol sensitivity of Ca2+ - and voltage-gated K+ (BK) channels. J Biol Chem 287: 20509–20521. DOI: 10.1074/jbc.M112.356261. [PubMed: 22474334]

Strøbæk D, Christophersen P, Holm NR, Moldt P, Ahring PK, Johansen TE, Olesen SP 1996. Modulation of the Ca2+-dependent K+ channel, hslo, by the substituted diphenylurea NS 1608, paxilline and internal Ca2+. Neuropharmacology 35:903–914. DOI: 10.1016/0028-3908(96)00096-2. [PubMed: 8938721]

Tano JY, Gollasch M, 2014. Hypoxia and ischemia-reperfusion: a BiK contribution? Am J Physiol Heart Circ Physiol. 307:H811–7. DOI: 10.1152/ajpheart.00319.2014. [PubMed: 25015960]

Taylor KC, Sanders CR, 2016. Regulation of KCNQ/Kv7 family voltage-gated K + channels by lipids. Biochem Biophys Acta. 1859(4):586–597. DOI: 10.1016/j.bbamem.2016.10.023.

Tomaselli G, Vallée M, 2019. Stress and drug abuse-related disorders: The promising therapeutic value of neurosteroids focus on pregnenolone-progesterone-allopregnanolone pathway. Frontiers in Neuroendocrin. 55:100789. DOI: 10.1016/j.yfrne.2019.100789.

Vallée M, Vitiello S, Bellocchio L, Hébert-Chatelain E, Monlezun S, Martin-Garcia E, Kasanetz F, Baillie GL, Panin F, Cathala A, Roullot-Lacarrière V, Fabre S, Hurst DP, Lynch DL, Shore DM, Deroche-Gamonet V, Spampinato U, Revest JM, Maldonado R, Reggio PH, Ross RA, Marsicano G, Piazza PV, 2014. Pregnenolone can protect the brain from cannabis intoxication. Science.343(6166):94–8. DOI: 10.1126/science.1243985. [PubMed: 24385629]

VilleMa E, Cho JS, 2015. Effect of aging on the vascular system plus monitoring and support. Surg Clin North Am. 95:37–51. DOI: 10.1136/bmjopen-2016-011031. [PubMed: 25459541]

Wang MD, Wanistrom C, Backstrom T, 1997. The regional brain distributation of the neurosteroids pregnenolone sulfate following intravenous infusion. J Steroid Biochem Mol Biol. 41:299–306. DOI: 10.1016/S0960-0760(97)00041-1

Wendt CC, 1991. The statistical distribution of the mean squared weighted deviation. Chemical Geology. 275–285. DOI:10.1016/0168-9622(91)90010-T.

Yan J, Aldrich RW, 2012. BK potassium channel modulation by leucine-rich repeat-containing proteins. Proceedings of the National Academy of Sciences. 09 (20) 7917–7922. DOI: 10.1073/pnas.1205435109.

Yuan C, O'Connell RJ, Jacob RF, Mason RP, Treistman SN, 2007. Regulation of the gating of BKCa channel by lipid bilayer thickness. J Biol Chem. 282:7276–7286. DOI: 10.1074/jbc.M607593200. [PubMed: 17209047]

Zhang J, Yan J, 2014. Regulation of BK channels by auxiliary γ subunits. Front Physiol. 5:401. DOI: 10.3389/fphys.2014.00401. [PubMed: 25360119]

Zhou Y, Lingle CJ 2014. Paxilline inhibits BK channels by an almost exclusively closed-channel block mechanism. J Gen Physiol. 144:415–440. DOI: 10.1085/jgp.201411259. [PubMed: 25348413]

Highlights

- Pregnenolone similarly constricts cerebral arteries of male and female mice.
- Pregnenolone action is independent of circulating and endothelial factors.
- Pregnenolone-induced constriction is mediated by BK channel inhibition.
- Pregnenolone inhibits BK channels independently of cell integrity.
- Pregnenolone inhibits BK channels independently of channel regulatory subunits.

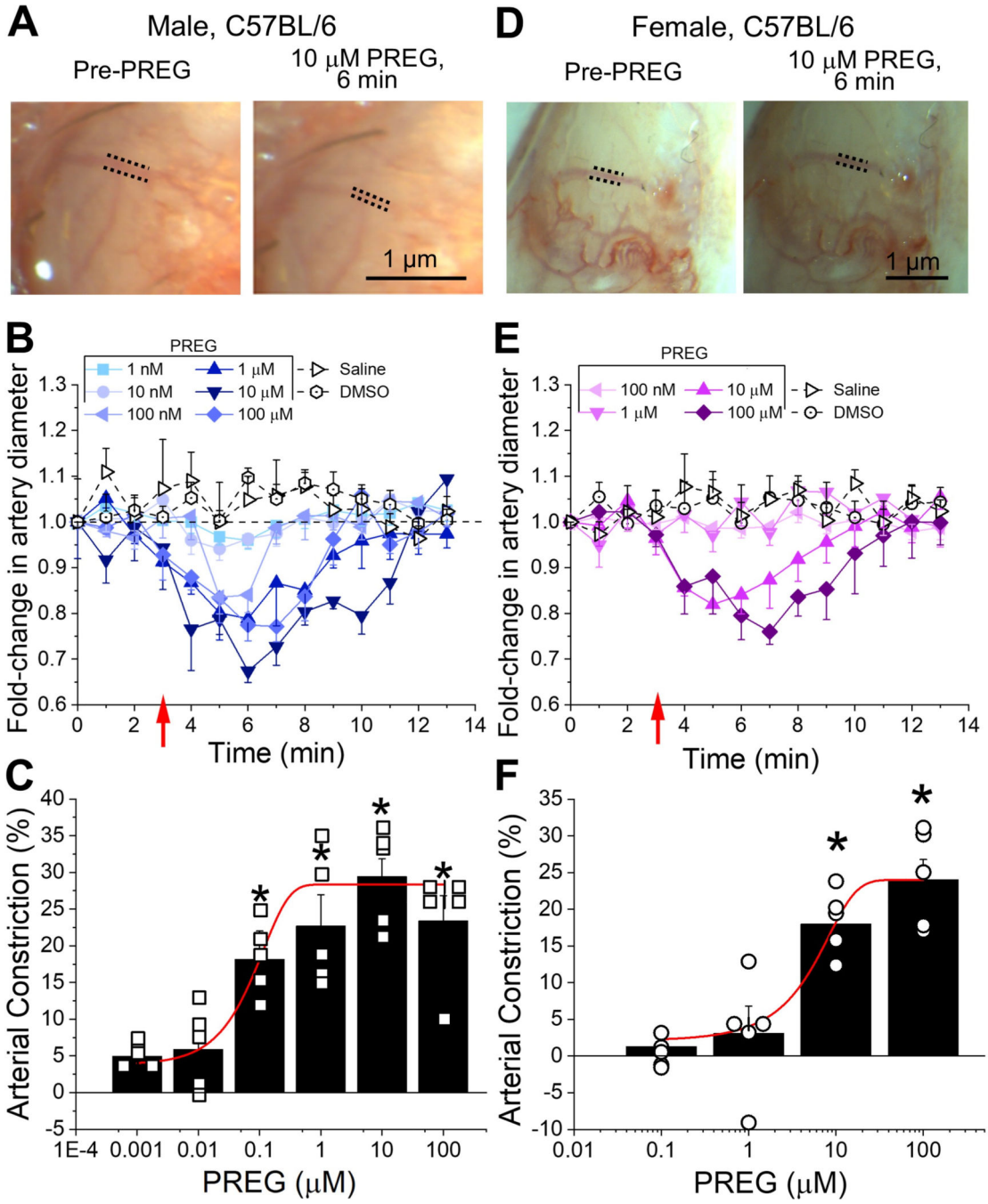

Figure 1. Pregnenolone constricts brain arteries of male and female mice, *in vivo*.

A. Cranial window images of C57BL/6 male MCA before any infusion (base) and 3 minutes after 10 μM pregnenolone (PREG) infusion *via* the carotid artery. Dashed lines are positioned along external MCA edges to highlight diameter changes by PREG. **B.** Averaged fold-changes in male MCA diameter for each minute of recording compared to baseline diameter determined from the image taken immediately prior to any infusion. A horizontal dashed line from 1 (y-axis), underscores no change in artery diameter. A red arrow indicates the beginning of infusion. Number of data points (n)=5–6 for each group, each data point

was obtained from a separate mouse. **C.** Averaged percentage of maximal artery constriction *in vivo* produced by each concentration of PREG in male C57BL/6 mice. A red line indicates Boltzmann fitting of data to obtain a concentration-response curve. Hollow squares are individual data points; each data point within a given PREG concentration was obtained from a separate mouse. **D.** Cranial window images of female C57BL/6 mouse MCA before any infusion (base) and 3 minutes after 10 μM PREG infusion. Dashed lines are positioned along the external MCA edges to highlight MCA diameter changes by PREG. **E.** Averaged fold-changes in female MCA diameter *in vivo* for each minute of recording via cranial window compared to baseline diameter determined from the image taken immediately before any infusion. A horizontal dashed line points at 1 (y-axis), i.e., point of no change in artery diameter. A red arrow indicates beginning of infusion. n=5 for each group; each data point was obtained from a separate mouse. **F.** Averaged percentage of maximal artery constriction *in vivo* produced by each concentration of PREG in female C57BL/6 mice. A red line indicated Boltzmann fitting to obtain a concentration-response curve. Hollow circles are individual points. Here, and in all figures: a) control perfusion included DMSO concentrations used to dissolve 100 μM PREG, and b) deviation from averaged value is shown as standard error. *Statistically significant difference compared to base (Mann Whitney U-test; $P<0.5$).

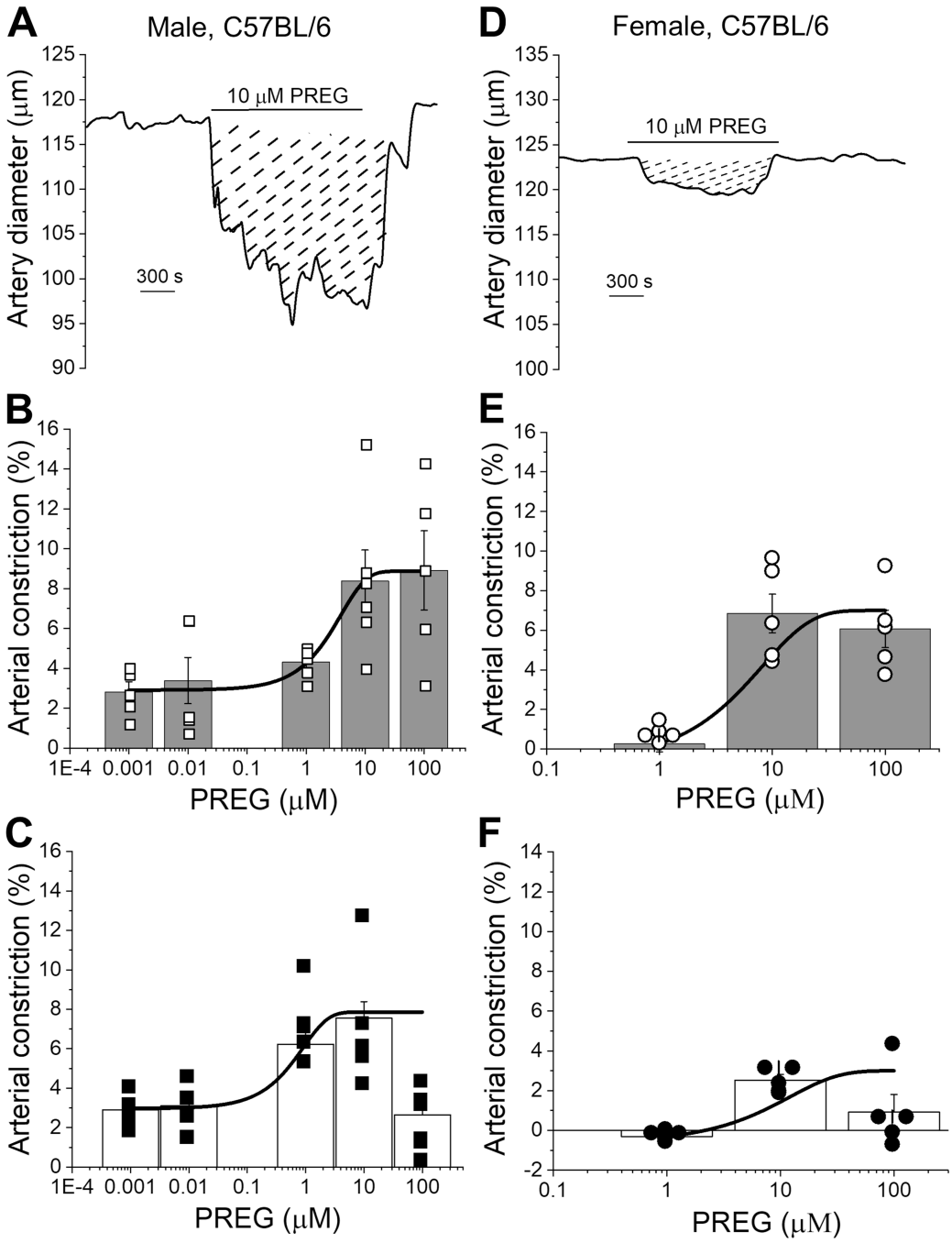

Figure 2. Pregnenolone is an endothelium-independent *in vitro* vasoconstrictor.

A. Diameter trace showing response to the application of 10 μM PREG in de-endothelialized pressurized MCA segments of C57BL/6 male mouse. Diagonal dashed lines highlight response (area under the curve) to 10 μM PREG. **B.** PREG-driven percent changes in endothelium-intact MCA of C57BL/6 male mouse. A black line indicates data fitted to a Boltzmann function to obtain a concentration-response curve. Hollow squares indicate individual points; n=5 for each concentration. Here and in **C, E-F,** each data point was obtained from a separate arterial segment. Within each group, individual data points were

obtained from separate mice**. C**. PREG-driven percent changes in de-endothelialized MCA of male C57BL/6 mouse. A black line indicates data fitted to a Boltzmann function to obtain a concentration-response curve. Black squares indicate individual points; n=5–6 for each concentration. **D.** Diameter trace showing responses to the application of 10 μM PREG in de-endothelialized MCA segment of C57BL/6 female mouse. Diagonal dashed lines highlight the area-under-the curve response to 10 μM PREG. **E.** PREG-driven percent changes in female MCA segments with intact endothelium. A black line indicates data fitted to a Boltzmann function (concentration-response curve). Hollow circles indicate individual points; n=5 for each concentration. **F.** PREG-driven percent changes in de-endothelialized MCA segments of C57BL/6 mice. A black line indicate data fitted to a Boltzmann function (concentration-response curve). Black circles indicate individual points; n=5–6 for each concentration. All individual records were recorded on separate artery segments.

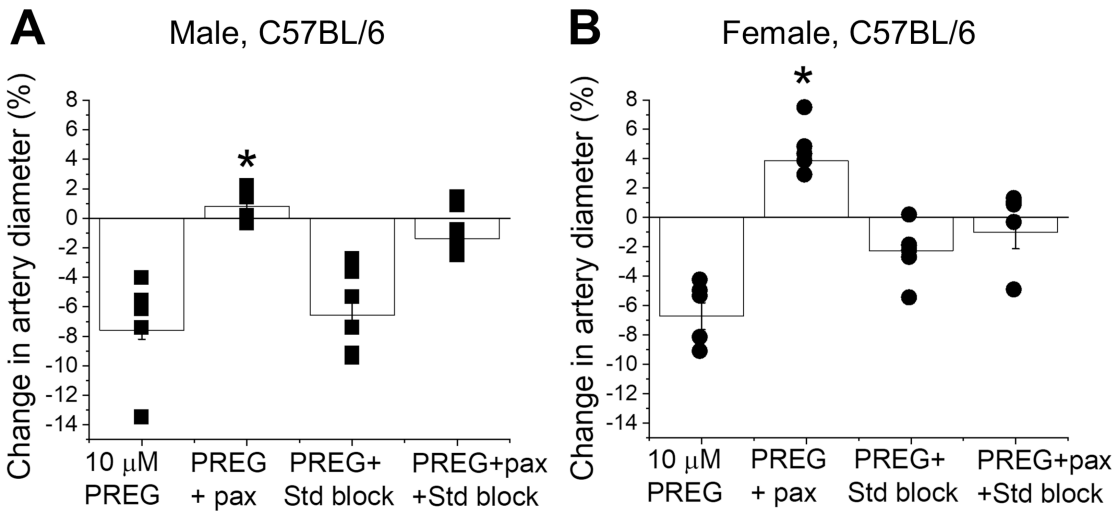

Figure 3. Simultaneous *in vitro* exposure to pregnenolone and blockers of either BK channels or known steroid receptors prevents this neurosteroid from constricting de-endothelialized middle cerebral arteries.

A. Comparison of percent changes in de-endothelialized MCA segments from C57BL/6 male mice in response to 10 μM PREG versus 10 μM PREG mixtures with either 1 μM paxilline, steroid receptor blockers (20 μM ketoconazole to block PXR, 33 μM MK-886 to block PPAR, and 20 μM MFA to block TRPM3), or their combination (i.e., PREG + paxilline + steroid receptor blockers). Black squares indicate individual points; n=5–6 for each group. Here and in B, individual data points within each experimental group were obtained from MCA segments of separate mouse donors. *Statistically significant difference from 10 μM PREG (P= 0.00114, Mann Whitney U-test). **B**. Comparison of percent changes in de-endothelialized MCA segments from C57BL/6 female mice in response to 10 μM PREG versus 10 μM PREG mixtures with either 1 μM paxilline, steroid blockers (described in **A** above), or their combination. Black circles indicate individual points; n=5 for each. *statistically significant difference from 10 μM PREG (P=0.00004, Mann Whitney U-test).

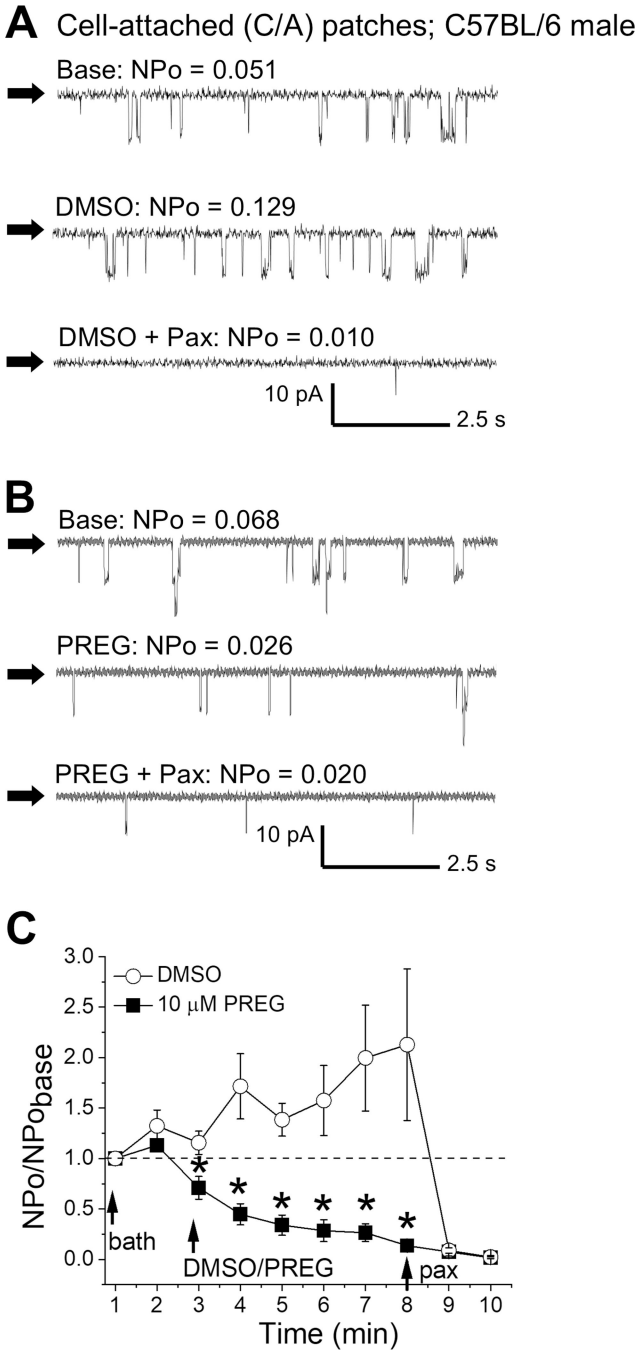

Figure 4. Pregnenolone inhibits BK activity in smooth muscle cells freshly isolated from mouse middle cerebral artery.

A. Representative cell-attached (C/A) records of BK opening during bath perfusion (top), DMSO perfusion (middle), or DMSO and 1 μM paxilline perfusion (bottom). Black arrows indicate baseline, channel openings are shown as downward deflections. Here and in B-C, all records were recorded at −30 mV. **B.** Representative C/A records of BK openings during bath perfusion (top), 10 μM PREG perfusion (middle), or 10 μM PREG + 1 μM paxilline perfusion (bottom). Black arrows indicate baseline, channel openings are shown as

downward deflections. C. Averaged data showing NPo/NPo_{basal} for each minute of recording. Dashed line at 1 (y-axis) indicates no change from basal channel activity. Black arrows indicate the start of perfusions. *Statistically significant difference from DMSO at each time-matched point ($P<0.05$, Mann Whitney U-test); n=5–8 for each group.

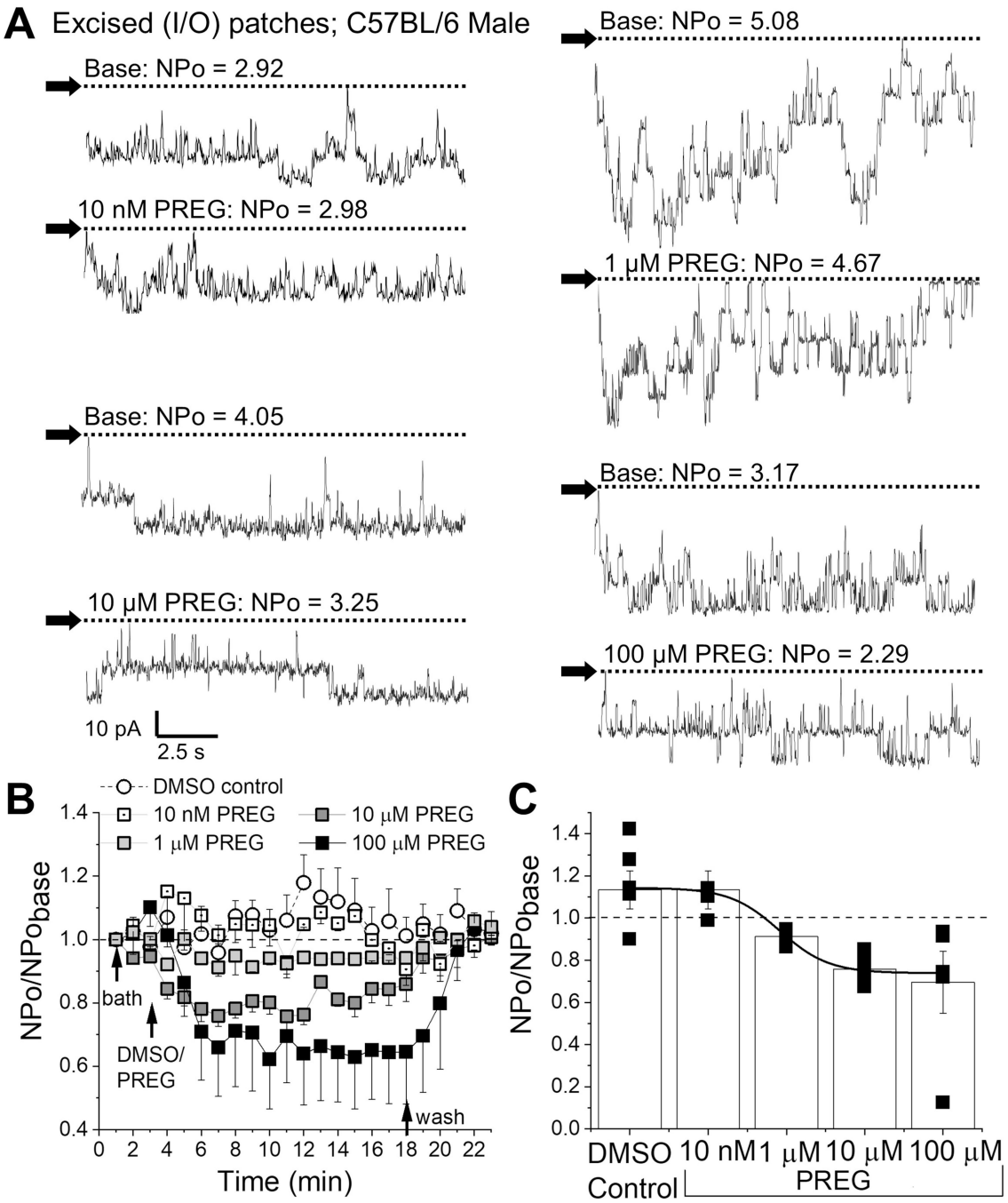

Figure 5. Pregnenolone inhibits BK activity independently of cell integrity.

A. Representative BK current recordings obtained from excised, inside-out (I/O) patches during bath perfusion (basal activity) and increasing amounts of PREG (10 nM-100 µM) in the perfusate. Horizontal dashed lines indicate the baseline. Black arrows indicate baseline, channel openings are shown as downward deflections. Here and in **B-C**, all records were recorded at +30 mV. **B.** Averaged data showing NPo/NPo_{basal} for each minute of recording per concentration of PREG, compared to time-matched DMSO-containing perfusion. Horizontal dashed lines indicate the baseline. Black arrows indicate changes in perfusion. **C.**

Averaged data highlighting maximal effects of increasing concentrations of PREG on BK channel activity. Black squares indicate individual points. A black line indicate data fitted to a Boltzmann function (concentration-response curve). A horizontal dashed line at 1 indicates no change from baseline activity; n=5 for each group.

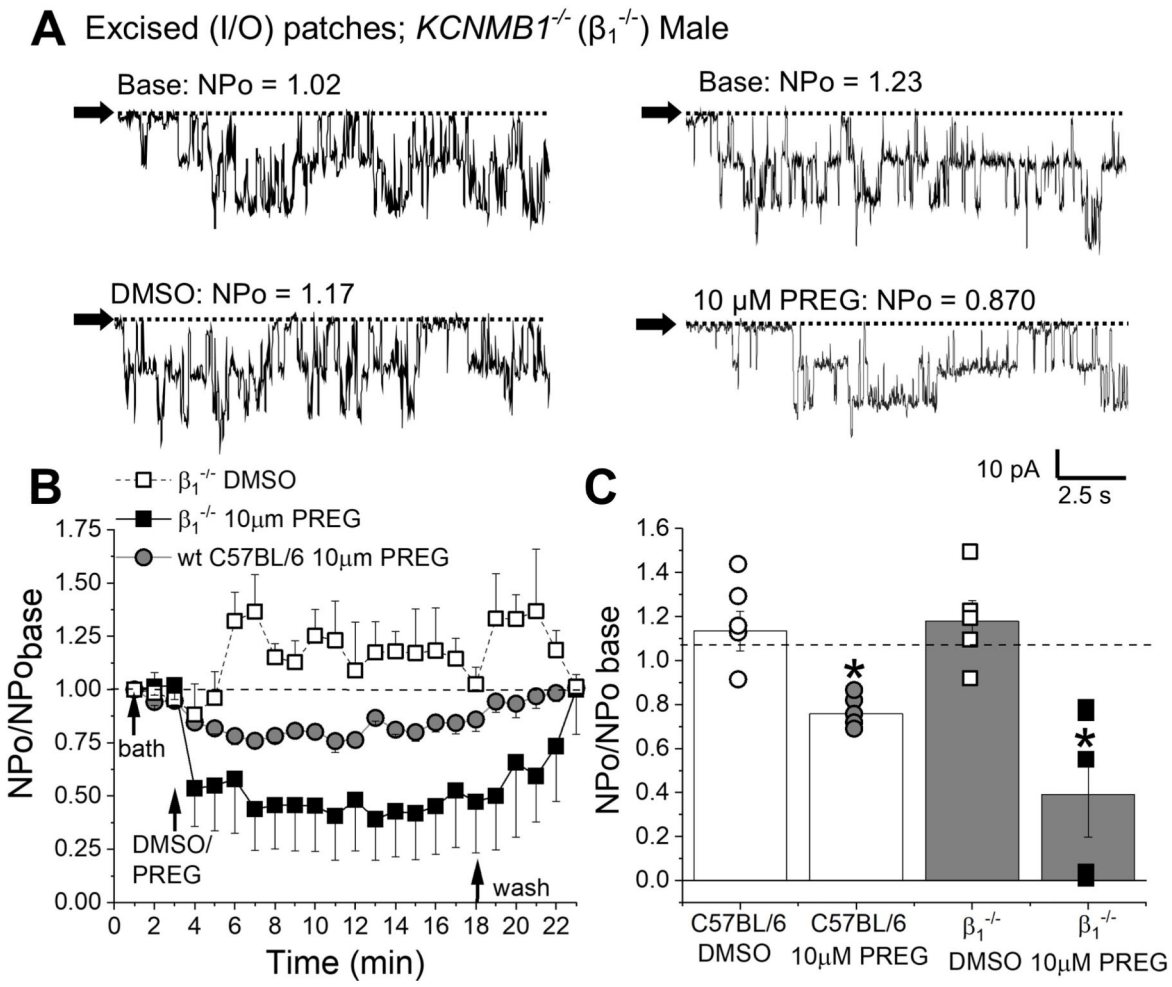

Figure 6. Pregnenolone inhibits BK activity in absence of BK β_1 subunits.

A. Representative BK current records obtained in I/O patches excised from membranes of *KCNMB1*$^{-/-}$ mouse MCA myocytes during bath perfusion (base; top left/top right), DMSO-containing perfusion (bottom left), 10 μM PREG perfusion (bottom right). Horizontal dashed lines and black arrows indicate the baseline. Channel openings are shown as downward deflections. Here and in **B-C**, all records were recorded at +30 mV. B. Averaged data showing NPo/NPo$_{basal}$ for each minute of recording and comparing the effect of 10 μM PREG on patches from MCA myocytes of *KCNMB1*$^{-/-}$, wt C57BL/6J, and *KCNMB1*$^{-/-}$ in DMSO exposed, time-matched records. Black arrows indicate changes in perfusion. A horizontal dashed line at 1 indicates no change from baseline. **C.** Comparison of the maximal effects of 10 μM PREG versus DMSO-containing control perfusion from wt C57BL/6J and *KCNMB1*$^{-/-}$ myocytes records. Hollow circles are individual points for wt C57BL/6J DMSO. Grey circles indicate individual points for wt C57BL/6J 10 μM PREG. Hollow squares indicate individual points for *KCNMB1*$^{-/-}$ in DMSO-containing perfusion. Black squares indicate individual points for *KCNMB*$^{-/-}$ at 10 μM PREG. Horizontal dashed line at 1 indicates no change from base. *Statistically significant difference from DMSO (P=0.01208, P=0.01208 for wt and *KCNMB1*$^{-/-}$, respectively; Mann Whitney U-test). There

were no statistically significant differences between the PREG groups; n=5–6 for each group.

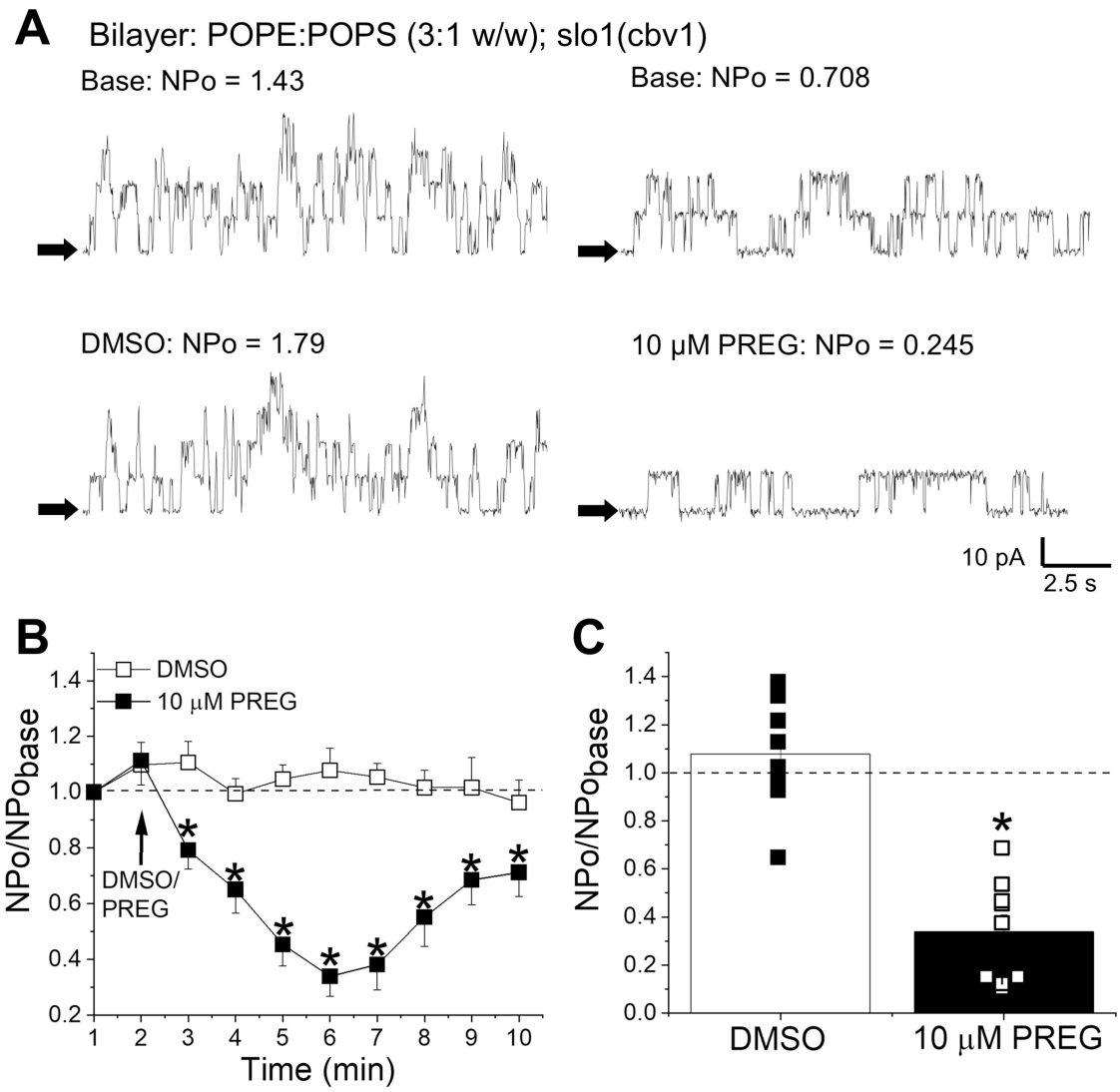

Figure 7. Pregnenolone inhibits the activity of homomeric slo1 channels reconstituted into artificial lipid bilayers.

A. Representative slo1 (cbv1 isoform) channel recordings obtained after incorporation of cbv1 into POPE/POPS (3:1 wt/wt) bilayers. Top traces are baseline recordings; bottom are traces after stock DMSO (bottom left) and stock PREG (bottom right) were added to both *cis* and *trans* chambers, for a final concentration of 10 μM PREG/DMSO. Channel openings are shown as upward deflections; black arrows indicate the baseline. Bilayers were bathed by bilayer recording solutions with 30 μM free calcium; all records were obtained at +30 mV. **B**. Averaged data showing NPo/NPo_{base} for each minute of recording, comparing 10 μM PREG versus DMSO time-matched controls. A black arrow indicates the time at which PREG/DMSO was added. A horizontal dashed line at 1 (y-axis) indicates no change from baseline activity. *Statistically significant difference from DMSO ($P<0.05$, Kruskal–Wallis test). **C.** Comparison of the maximal effect of 10 μM PREG to DMSO. Black squares indicate individual points for DMSO; hollow squares indicate individual points for PREG. A horizontal dashed line at 1 (y-axis) indicates no change from baseline activity. *Statistically significant difference from DMSO ($P= 0.01791$; Kruskal–Wallis test); n=9 for each.

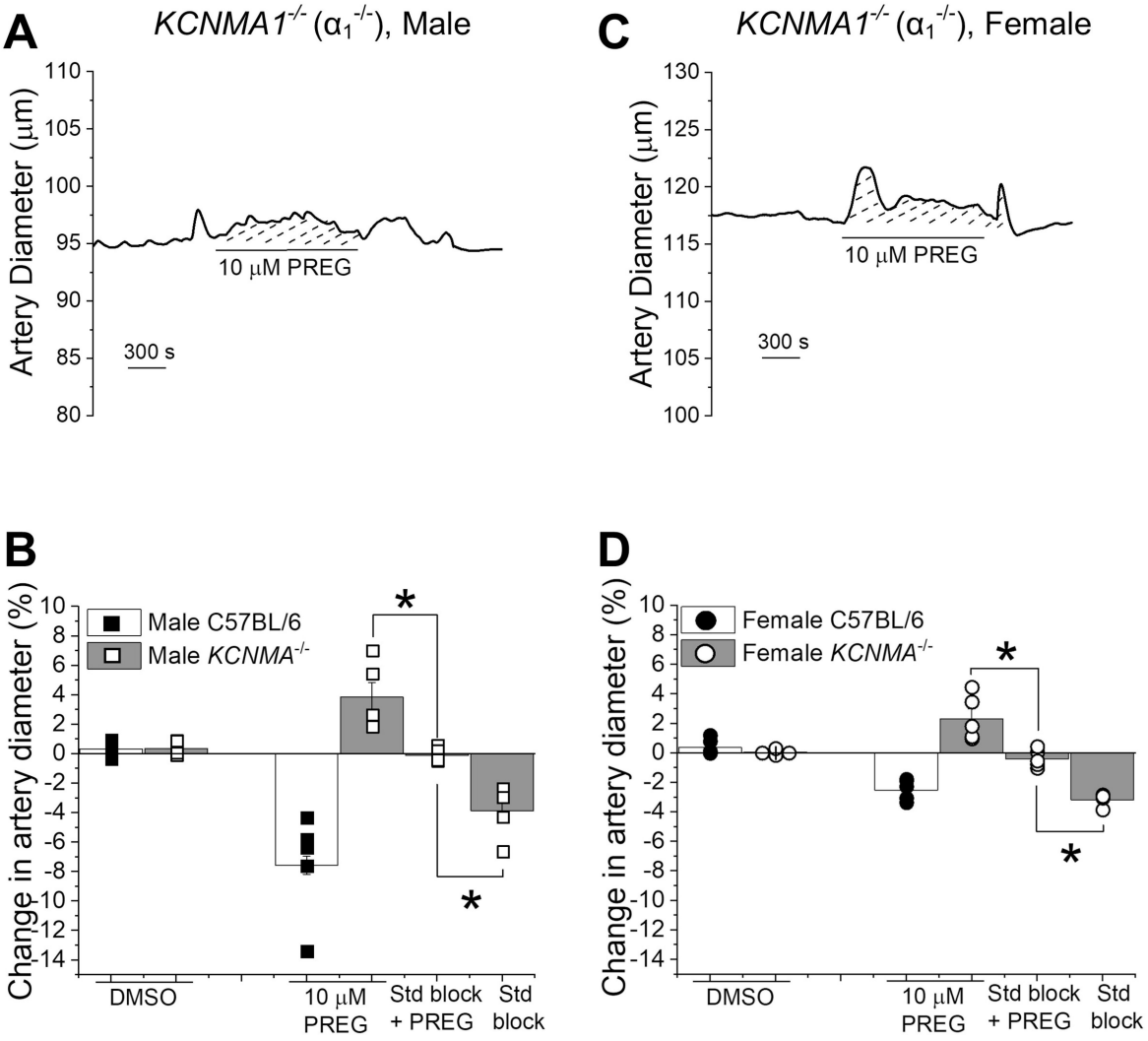

Figure 8. The absence of BK α subunits (slo1 proteins) prevents pregnenolone from constricting middle cerebral arteries.

A. Diameter trace showing the response of pressurized, de-endothelialized MCA segment from *KCNMA1*$^{-/-}$ male mouse to 10 μM PREG.

B. Comparison of arterial responses to 10 μM PREG in absence and presence of the steroid block, and DMSO in wt C57BL/6J and *KCNMA1*$^{-/-}$ male mice. Black squares indicate individual responses from male wt C57BL/6J; hollow squares indicate individual responses from male *KCNMA1*$^{-/-}$ mice. *Statistically significant difference from 10 μM PREG in presence of steroid receptor blockers (P= 0.00439, P= 0.00169 from left to right, Kruskal–Wallis test). C. Diameter trace showing the response of in pressurized, de-endothelialized MCA segment from *KCNMA1*$^{-/-}$ female mouse to 10 μM PREG. **D.** Comparison of the arterial response to 10 μM PREG in absence and presence of the steroid block, steroid receptor blockers, and DMSO in wt C57BL/6J versus *KCNMA1*$^{-/-}$ female mice. Black circles indicate individual responses from female wt C57BL/6J; hollow circles indicate individual responses from female *KCNMA1*$^{-/-}$ mice. *Statistically significant difference from 10 μM PREG in presence of the steroid block (P= 0.00607, P= 0.00002 from left to

right, Kruskal–Wallis test); n=5 for each group. Each data point was obtained from a different MCA segment; all data-points within each group were obtained from separate mouse donors.